ESTABLISHMENT OF HIGH-THROUGHPUT TECHNIQUES FOR STUDYING STARCH FUNCTIONALITIES

by

Miguel Angel Alvarez Gonzales

A Thesis

Submitted to the Faculty of Purdue University

In Partial Fulfillment of the Requirements for the degree of

Master of Science

Department of Food Science

West Lafayette, Indiana

August 2019

THE PURDUE UNIVERSITY GRADUATE SCHOOL
STATEMENT OF COMMITTEE APPROVAL

Dr. Yuan Yao, Chair
Department of Food Science
Dr. Bruce Hamaker
Department of Food Science
Dr. Clifford Weil
Department of Agronomy

Approved by:
Dr. Arun K. Bhunia
Head of the Graduate Program

Dedicated

to

my family

TABLE OF CONTENTS

LIST OF TABLES

LIST OF FIGURES

LIST OF ABREVIATIONS

1D ^{1}H NMR	Proton NMR
^{31}P NMR	Phosphorus-31 NMR
AM	Amylose
AP	Amylopectin
CCVJ	9-(2-carboxy-2-cyaovinyl)-julolidine
cP	Centipoise
d.s.b	Dry starch base
D_2O	Deuterium oxide
DCVJ	9-(2,2-dicyanovinyl) julolidine
DMSO	Dimethyl sulfoxide
DSC	Differential scanning calorimeter
FDA	Food and drug administration
FTC	Freeze-thaw cycle
FTIR	Fourier-transform infrared spectroscopy
g	Gram
G’	Shear storage module
G”	Loss module
H_2SO_4	Sulfuric acid (H_2SO_4),
HTP	Hydrothermal transition properties
LE	Locally excited state
M	Molar
mg	Milligram
min	Minute
ml	Milliliter
mm	Millimeter
MS	Molar substitution
Na_2HPO_4	Sodium phosphate dibasic
NaH_2PO_4	Monobasic sodium phosphate
NCS	Normal corn starch

NIR	Near-infrared
NMR	Nuclear magnetic resonance
ºC	Celsius degrees
PCR	Polymer chain reaction
PdI	Polydispersity index value
PO	Propylene oxide
$POCl_3$	Phosphoryl chloride
RFU	Relative fluorescence units
RPM	Revolutions per minute
RVA	Rapid viscosity analyzer
s	Second
s.b.	Starch base
SKS	Single kernel sampling
SO_2	Sulfur dioxide
STMP	Sodium trimetaphosphate
STPP	Sodium tripolyphosphate
TC	Temperature cycle
TICT	Twisted intramolecular charge transfer state
UV/Vis	Ultraviolet/visible
WCS	Waxy corn starch
αCD	α-cyclodextrin
β-CD	β-cyclodextrin
γ-CD	γ-cyclodextrin
µL	Microliter
µm	Microgram
µM	Micromolar

ABSTRACT

Author: Alvarez Gonzales, Miguel, A. MS
Institution: Purdue University
Degree Received: August 2019
Title: Establishment of High-Throughput Techniques for Studying Starch Functionalities.
Committee Chair: Dr. Yuan Yao

Maize is one of the top sources of food starch. Industrial use of starch is mostly in its native form and used due to their functional and structural properties. Native starch properties and functionalities have been altered using chemical. An alternative for the development of native starch substituents with desirable starch properties is the use of mutagenesis techniques to increase genetic variation in maize kernels. With this approach, a highly diverse library of native starches with different properties are produced. Traditional analysis of the functional and structural properties requires generous amounts of material as well as a time-consuming and costly breeding process to obtain enough kernels. To address this difficulty, high-throughput techniques are proposed for studying starch properties and functions which includes a 1) single kernel sampling method for the isolation of milligrams of starch, and techniques for studying starch based on functional properties, 2) retrogradation and 3) shear resistance, using low-volume low-concentration starch pastes.

First, three mechanical approaches were evaluated for the collection of endosperm samples from individual kernels: razor blade, 1.5 mm drill bit, and trephine bur. Furthermore, two methods for the isolation of crude starch from endosperm samples (steeping method and combination of proteases and sonication) were compared. In this study, the mechanical approaches were evaluated using the recovery rate, throughput, and germination rate of sampled kernels. Moreover, yield determination, particle size distribution, and morphological evaluation using a light microscope were performed on crude starch isolated from the endosperm samples. The use of trephine bur to collect endosperm samples and isolation of crude starch using protease digestion and sonication showed the best combination for a high-throughput setting.

Second, a high-throughput technique using milligram sample for the screening of retrogradation-resistant starch was evaluated by comparing two spectrophotometric techniques: turbidity method and molecular rotor (MR). MRs are fluorescent probes with high sensitivity to

the viscosity of their environment, polarity of the media, molecular crowding, and free volume. After excitation, MRs relax through rotational movement and reduces the emission of fluorescence. In this study, hydroxypropylated waxy corn starch (WCS) and hydroxypropylated normal corn starch (NCS) were used and their retrogradation kinetics was compared with retrogradation kinetics of native WCS and NCS.

It was found that the molecular rotor 9-(2-carboxy-2-cyaovinyl)-julolidine (CCVJ) was effective to sense changes during slow retrogradation of amylose-containing starch pastes. Development of elastic modulus of retrograded NCS pastes obtained from dynamical rheology showed high correlation with the development of fluorescence intensity of the CCVJ. Furthermore, rate of retrogradation using fluorescence intensity was affected by the introduction of a retrogradation inhibitor, hydroxypropyl groups. Accelerated retrogradation of low-concentration WCS pastes was measured using the turbidity method and fluorescence intensity of CCVJ in a microplate. Accelerated retrogradation was performed by subjecting the low-concentration WCS pastes to six freeze-thaw cycles of -20 ºC for 1 hour and 30 ºC for 1 hour. Overall, development of turbidity resulted in the more sensitive technique to detect rate of retrogradation of amylopectin-containing starch.

The last part of this research studied the use of CCVJ as a technique to identify shear-resistant starch in starch slurries using milligram sample. For this purpose, WCS was cross-linked with sodium trimetaphosphate (STMP) and phosphoryl chloride ($POCl_3$). Low-volume starch slurries having CCVJ were prepared ranging from 0.5% to 1% starch concentration in a 96-well PCR plates and subjected to heat and shear treatments. It was found that fluorescence intensity measured in native WCS pastes were the lowest. Furthermore, fluorescence intensity of the CCVJ in the gelatinized starch increased as the amount of cross-linker increased in the cross-linked WCS. After shear treatments, the same trend in fluorescence intensity increase was recorded in all the crosslinked WCS. Results obtained using fluorescence intensity were compared with rapid viscosity analyzer (RVA) and images from microscope. Results obtained from both techniques corroborated the findings using fluorescence intensity.

In general, the findings of this research provide new insights into the possibilities of developing a high-throughput screening platform of milligram starch sample based on their physical properties.

CHAPTER 1. LITERATURE REVIEW

1.1 Introduction

The production of starch is predicted to grow due to their extensive use not only in the food industry but also the paper, textile, pharmacy, and chemical industry. Sales of starch were expected to reach $77.4 billion by 2019 (Business Research Company, 2016). Starch in its native form was reported to represent 74% as primary use for industrial purposes, followed by hydrolyzed and modified starches (Business Research Company, 2013). Starch is obtained from a variety of botanical sources, but maize is one of the top sources. Starch is incorporated to food systems which benefit from its inherent diverse functional properties. In order to be incorporated in food stuffs, starch needs to provide a wide range of attributes and withstand a range of processing conditions (BeMiller, 2019). However, native starches have few of the desired characteristic and are very susceptible to heat, shear, and recrystallization. These defects are addressed by modifying starch through genetical, chemical, physical, or enzymatic methods that enhance native starches properties and increase their functionalities.

Starch is composed of two polysaccharides: amylose (AM) and amylopectin (AP). The variation in their molecular structures, ratio, chemical composition, and molecular organization confers all the properties that starch exhibits (Wiesenborn et al., 1994; Vamadevan & Bertoft 2015). Moreover, these variations occur in different botanical sources and within botanical source. For this reason, it is necessary to understand starch structure at distinct levels of organization to predict its physicochemical properties.

The increase in the demand of “organic” and natural ingredients is continuously growing. The demand to eliminate “artificial” products creates a new challenge to the food industry to replace the chemically modified ingredients and replace them with natural substituents. However, this task it is not easy and requires a lot of effort not only of the food processors but their partners as well. The development of new mutant lines of maize is showing promise for the development of new native material with the idea of finding cost-efficient natural substituents. Protein, fiber, and gums have been studied as natural substituents of starch. However, the disadvantage of the use of these materials is the cost and new properties that can be incorporated which are not

desirable. The finding of a promising solution is the identification of novel starch with comparable properties to those of modified starches that can be exploited in an industrial setting.

In the present work, the overall goal was to develop new high-throughput methods for the screening of starch obtained from mutagenesis approaches or germplasm library based on desired physicochemical properties or enhanced functionalities. Spectrophotometric methods and the use of molecular rotors helped design novel approaches for the study of two starch properties. These new methods were compared with conventional methods of analysis. Finally, the combination of the high-throughput techniques with a single kernel analysis assures the development of a platform to screen corn kernels to accelerate the selection of novel starch materials.

1.2 Clean label movement

The clean label movement has arisen as health-conscious consumers demand simple names, minimal use of manufacturing aids, inclusion of natural ingredients and being free from GMO, gluten, allergens, and artificial or synthetic components (Finamore, 2017). Although the development of modified starches has led to the creation of new products, the introduction of the "clean label" trend represents a challenge for food companies and their partners to search for new natural ingredients (Asioli et al., 2017). Moreover, the reduction of the "unhealthy" and "unfamiliar" components of the food system is requiring food companies to develop techniques to improve functionalities of native starches by physical modification, thermal treatment, and selective crop breeding (McDonagh, 2012).

This demand for "natural" and healthy products represents an opportunity to explore new techniques and develop natural starch substituents that are cost-efficient and can replace the use of modified starches in food stuffs.

1.3 Genetic modification of corn

With the development of industrial farming and the growing of the global population, a demand for higher yields has led to development of maize hybrids. However, the genetic variability of corn is suppressed with the development of new hybrids; thus, leading to the need to increase the genetic variation to enhance desirable traits such as yield, quantity and quality of starch, protein, oil, and other aspects such as pericarp thickness or kernel hardness (Darrah,

McMullen, & Zuber, 2019). The development of new techniques to increase mutagenesis, genetic transformation, and genome editing can be used to modify the genetic information of maize and obtain plants with different genetic backgrounds (Cabrera-Ponce, Valencia-Lozano, & Trejo-Saavedra, 2019).

1.3.1 Increasing genetic variation of corn

Mutagenesis has been used to induce mutations and increase the genetic variation in maize. The approaches to induce mutation in maize include the use of 1) transposons, which insert a *Mutator* element and activator/dissociation element in the genome to induce mutation of genes; 2) other techniques that do not involve transposons, which uses chemical and physical mutation of the genome; and 3) phenocopying strategies, which silence gene expression by the use of double-stranded RNAs (RNAi) (Weil & Monde, 2007; Cabrera-Ponce et al., 2019)

With the current use of mutagens, a high number of mutant lines have been produced and an effective approach to identify mutant lines with starch possessing desirable properties and their corresponding genotypes is highly needed. Furthermore, the combination of mutagens and breeding techniques will result in an increase in the effectiveness and efficiency of selection of several quantitative traits with the goal of creating or identifying novel native starches that show the functionalities of chemically modified starch. However, two fundamental issues arise: 1) vitality of seed after analysis or screening needs to be preserved; and 2) limitation in the amount of material obtained. With these two limitations, screening techniques are needed that can enable identification of novel native starch and advance fundamental research of starch.

1.3.2 Single corn mutant effects

Single mutant maize with known recessive genes that alter the fine structure and ratio of starch components in the endosperm have been identified (Table 1.1). In addition, the effect of recessive genes in the triploid endosperm also depends of the genetic background (Wang, 1992). Lastly, combination of recessive genes may result in additional variations to both structure and properties of the starch components (Boyer & Liu, 1985; Ninomya et al., 1989; Shannon, Garwood, & Boyer, 2009).

Table 1.1 Characteristics of maize mutant with single recessive gene

Mutant genotype	Description	Reference
AM-extender (*ae*)	High apparent amylose content ranging from 50 to 80%.	Banks, Greenwood, & Muir, 1974
waxy (*wx*)	Epistatic to all other known recessive genes for blocking amylose accumulation.	Wang, 1992 ; Inouchi et al., 1991
brittle-1 (*bt1*)	Higher sugar content at the expense of starch accumulation.	Ninomya et al., 1989
shrunken-2 (*sh2*)	Reduced starch content to about 30% of the normal amount with dramatically increased sucrose content.	Holder, Glover, & Shannon, 1974; Dickinson & Preiss, 1969
sugary 1 (*su1*)	Accumulation of phytoglycogen to 25% or more of the kernel dry weight.	Ninomya et al., 1989; Yeh & Yeh, 1993; Holder et al., 1974
dull (*du*)	Increased AM content compared with normal corn starch.	Holder et al., 1974; Ikawa et al., 1981; Boyer & Liu, 1985

Source: Wang (1992)

1.4 Starch and starch composition

Starch is a major component of energy storage in maize and is mainly isolated from the corn kernel by the wet-milling process (BeMiller, 2019). Starch is a porous semi-crystalline and water-insoluble granule and is composed of two different polysaccharides. AM is a linear polymer, is composed by glucose units linked mainly by α-1,4 glycosidic bonds, and presents few ramifications in the position α-1,6. On the contrary, AP, with a molecular weight ranging from 10^7 to 5×10^8 Da (Ratnayake & Jackson, 2008; Hamaker, Tuncil, & Shen, 2019), is a highly branched polymer of glucose units linked by α-1,6 glycosidic linkages and also linear branch chains of glucose linked by α-1,4 glycosidic bonds (Matignon & Tecante, 2017). Each AP chain may contain an average of 6-100 α,1-4 linked anhydroglucose residues (Ai & Jane, 2018). The composition of each polymer varies in corn starch, for example: NCS contains ~25% AM while the mutant WCS may contain >90% AP.

1.4.1 Starch granule architecture

Distinct levels of organization were found in the starch granule. Adjacent AP chains are associated into a double-helical crystallite and packed mostly in two different patterns: the A-type and the B-type polymorph with monoclinic unit cell and hexagonal unit cell, respectively (Buléon

et al., 1998). The double helices are packed into lamellas structure (Angellier-Coussy et al., 2009) and the AP lamella into spherical blocklets with a diameter of 20-500 nm (Gallant, Bouchet, & Baldwin, 1997). The blocklets are organized into hard and soft shells that allows the occurrence of growth rings in the starch granule (Ai & Jane, 2018). AM and AP are organized in amorphous and crystalline domains, respectively, arranged in alternating concentric rings that create a semi-crystalline environment within the granule (Ratnayake & Jackson, 2008).

Variation of the starch physical properties are due the molecular composition, chemical composition, and molecular organization which varies between botanical sources and within botanical (Wiesenborn et al., 1994; Vamadevan & Bertoft 2015). Fine structure of AP (i.e. chain length, distribution of chain lengths, and ratio of short to long chains), AM structure; and AM-AP ratio can be affected by the mutation of the starch biosynthetic enzymes. Moreover, the use of chemical mutagenesis promotes changes in the maize genotype, that may affect starch properties relevant to the food industry.

1.5 Starch properties in water: Gelatinization, pasting, and retrogradation.

Starch is the main ingredient in food products and is used due to its hydrothermal transition properties. When subjected to heating in presence of water, the starch granule undergoes a series of changes that are responsible for its food-industry relevant properties such as gelatinization, pasting, and retrogradation (Sullivan and Johnson, 1964; BeMiller & Whistler, 2009; Biliaderis, 2009).

1.5.1 Gelatinization

Gelatinization is the process by which the semi-crystalline structure of the native granule is lost due to rapid hydration during heating (BeMiller, 2019). Starch granules are rapidly hydrated when added to aqueous system. Heating the aqueous starch dispersion increases hydration of the starch granule. Water acts as plasticizer and disrupts hydrogen bonds first in the amorphous regions of the granule with a change of shape, and second in the crystallites when the granule swells even more due to excessive heating (BeMiller, 2019). Heating starch granules in presence of water until melting of crystallites increases the volume of the granule and a loose structure is formed (Ai & Jane, 2018). This process is mainly responsible for the inherent hydrothermal transition properties of native starches. The difference in the fine structure and organization of starch molecules inside

the starch granule between botanical sources and within botanical source is reflected in the different gelatinization properties (Jane et al., 1999).

1.5.2 Pasting

An excess of heating and shearing of starch granules in excess water results in more swelling, leaching of the starch molecules, and disruption of the granule (BeMiller, 2019). As a result, a viscoelastic mass (i.e., paste) is formed consisting of a continuous phase that is a molecular dispersion of starch polymers and a discontinuous phase of swollen granules, granule ghosts, and granule fragments (BeMiller, 2011). Consequently, solubility of the granules, development of viscosity, and other properties related with the structure and organization of starch molecules inside the swollen starch granule such as texture and transparency are developed (Biliaderis, 2009).

1.5.3 Shear resistance

Shear resistance is the property of the starch granule to withstand severe heat and shear processing conditions. The rupture of the granules during pasting of starch are of high importance in developing food-relevant properties. When the granule is swollen, a rapid development of viscosity in the paste can be measured. Thereafter, rupture of the granules will result in a paste with low viscosity, low texture, stringy, and cohesive (Tattiyakul & Rao, 2000). Fine structure of AP affects gelatinization; Jane et al. (1999) reported a high pasting temperatures in starch dispersions of *ae* waxy which contain very-long AP chain than waxy starch. They suggest that very-long chain AP will hold the integrity of starch granules during heating and shearing, conferring shear-resistance to their granules.

1.5.4 Retrogradation

After gelatinization, reorganization of starch polymers into a water-insoluble semi-crystalline structure has been recorded, retrogradation. Starch retrogradation is divided into two phases short-term and long-term retrogradation (Jacobson & BeMiller, 1998). Short retrogradation occurs immediately when the paste cools down and involves network formation among AM molecules (Fredriksson et al., 1998; Wang et al., 2015); this process can take up to 48 hours (BeMiller, 2011). Long-term retrogradation is a much slower process and may take several weeks for completion (Ring et al., 1987; Fredriksson et al., 1998); AM-AM, AM-AP, and AP-AP interaction govern this phase (Wang et al., 2015).

Recrystallization of AM and AP is described as a three-step process which includes formation of critical nuclei (nucleation), growth of crystals from the nuclei formed (propagation), and continuous slow growth or crystal perfection (maturation) (Zhou et al., 2010); the first two affect the speed of crystal formation (Eerliengen, Crombez, & Delcour, 1993). Furthermore, physical changes are accompanied with starch retrogradation such as increased viscosity and turbidity of pastes, gel formation, exudation of water and increase in crystallinity with the appearance of B-type crystal polymorphs (Hoover et al., 2010).

Jacobson, Obanni, and Bemiller (1997) described that the rate of retrogradation depends of structure of AM and AP, ratio of AM to AP, temperature, starch concentration, botanical source of starch, and presence and concentration of other ingredients. The rate of retrogradation can be accelerated when the temperature of storage is cycled between the temperature of nucleation and temperature of propagation which promotes growth of crystalline regions and perfection of crystallites. (Jacobson & BeMiller, 1998; Silverio et al., 2000; and Zhou et al., 2010). Different temperature cycling has been used successfully to accelerate rate of retrogradation of starch pastes. Freeze-thaw cycling has been demonstrated to be an efficient method to study retrogradation in a short period of time (Jacobson & BeMiller, 1998).

1.6 Enhancement of starch properties

Genetic, chemical, physical, and enzymatic modifications can be used to enhance hydrothermal transitional properties of native starches and improve their functionalities. Chemical modifications are the most common methods to enhance properties of starch and improve their functionalities by stabilizing the granule with the introduction of chemical bonds at random locations (Tattiyakul & Rao, 2000). Among the chemical modifications, crosslinking and stabilization (hydroxypropylation) are the two mostly used to provide tolerance to processing conditions and prevent overcooking and to modify properties to prolong product stability, respectively (BeMiller, 2019).

1.6.1 Cross-linking of starch

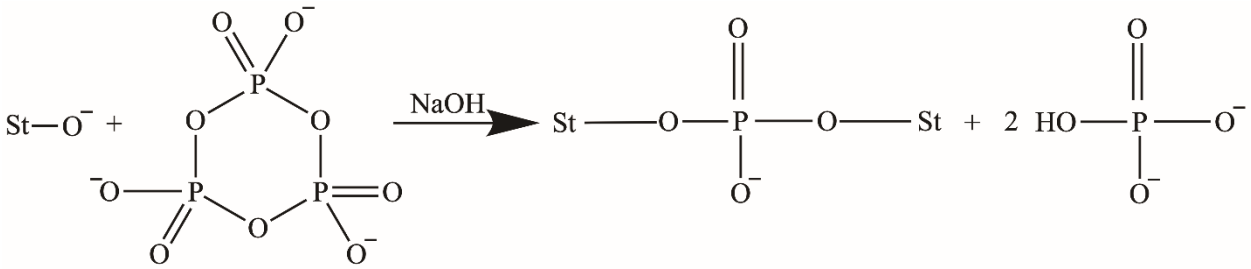

Figure 1.1 Chemical cross-linking of starch with sodium trimetaphosphate

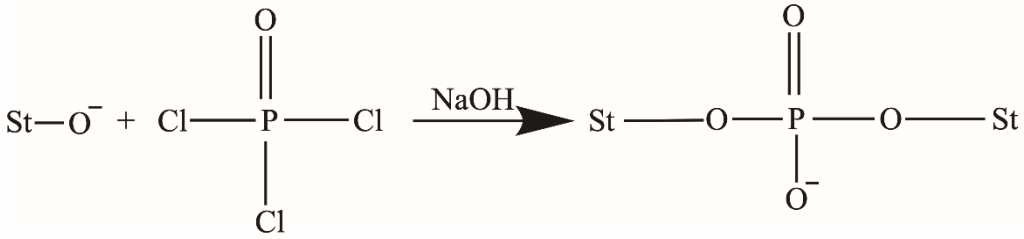

Figure 1.2 Cross-linking reaction of starch with phosphorus oxychloride

Cross-linking of starch is usually accomplished by reacting it with monosodium phosphate, sodium trimetaphosphate (STMP) (Figure 1.1), phosphoryl chloride ($POCl_3$) (Figure 1.2), epichlorohydrin, a mixture of adipic and acetic anhydrides, or a mixture of succinic anhydride and vinyl acetate (Hirsch & Kokini, 2002).

The use of a crosslinker has been regulated by the Food and Drug Administration (FDA) and no more than 1% (weight of dry starch) of STMP or no more than 0.1% of $POCl_3$ can be used (BeMiller & Whistler, 2009). Introduction of phosphate linkages into starch granule increases the average molecular weight (Rutenberg & Solarek, 1984), restricts swelling, and reduces granule rupture, loss of viscosity, and formation of a stringy paste during cooking (Woo & Seib, 1997).

1.6.2 Stabilization of starch

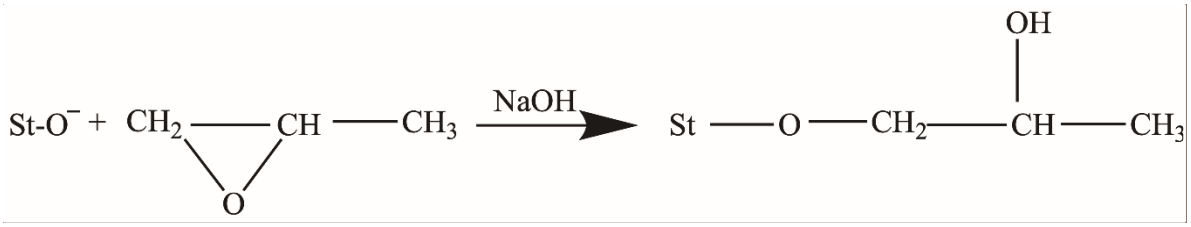

Figure 1.3 Chemical stabilization of starch with propylene oxide

Stabilization of starch involves either the esterification or etherification of the granules. The main objective of this chemical modification is to create products whose hot paste and gels exhibit less retrogradation and syneresis (BeMiller, 2019). The reaction of stabilization is performed in a basic medium with the addition of a salt, usually sodium sulfate to repress swelling and prevent pasting (Gray & BeMiller, 2005), followed of the addition of the hydroxyalkyl, mainly propylene oxide (Rutenberg & Solarek, 1984) (Figure 1.3).

1.6.3 Increasing genetic variability for the modification of starch properties

One alternative to chemical modification is the identification of native starches with improved native-starch functionalities. For example, fine structure of AP (i.e. chain length, distribution of chain lengths, and ratio of short to long chains), AM structure; and AM-AP ratio can be affected by the mutation of the starch biosynthetic enzymes. Vamadevan & Bertoft (2018), reported that AP with longer external chain length and longer inter-block chain length favors retrogradation; while AP with shorter chains counteract retrogradation. Furthermore, AM chain length will also affect rate and extent of retrogradation. Precipitation were found to occur with short-chain AM (DP<110), whereas long-chain AM (DP>1100) were found to form gels after cooling of pastes (Jankowski, 1992).

New mutagenesis techniques of maize ensure the increase in genetic variation resulting in new mutant plants with native starch that may offer diverse functionalities. After identification of individuals having desired novel starch, these individuals can be later introduced in breeding programs to capture the desired attributes with commercial maize lines. However, the identification of individual with desirable traits has two limitans: 1) the vitality of seeds needs to be kept, and 2) limited amount of material is available for analysis. Classic analytical methods of starch properties use bulk kernels, require large amount of materials, and need long time to collect, process, and analyze data; therefore, tracking the properties of starch from individual kernels is difficult. Evidently, a high-throughput starch screening platform based on starch analysis of individual kernels is necessary.

1.7 Conventional methods for studying starch properties.

1.7.1 Conventional methods for studying gelatinization.

Measurement of starch gelatinization is accomplished by measuring the temperature range and the degree of gelatinization. The temperature range is studied by polarized-light hot-stage microscopy, which defines gelatinization temperature as the temperature at which more than 98% of granules lose birefringence (Collison, 1968). Differential Scanning Calorimeter (DSC) measures the temperature and enthalpy during gelatinization (Zhong & Sun, 2005). The degree of gelatinization can also be measured using the rate of enzyme-catalyzed hydrolysis, X-ray diffraction, molecule dissolution, and dye absorption (Ratnayake & Jackson, 2008).

1.7.2 Conventional methods for studying paste properties and shear resistance.

The mostly used conventional method to determine paste properties (including shear resistance of starch) is the use of rapid viscosity analyzer (RVA). The measurement of paste properties is based on the measurement of viscosity of a starch paste and recording of changes of viscosity during heating and cooling with constant stirring (Wiesenborn et al., 1994). From the RVA profiles, several paste properties can be obtained such as pasting temperature, peak viscosity, hot paste viscosity (trough), final viscosity, breakdown, and setback (BeMiller, 2011) (Table 2). Breakdown is an indicator of how susceptible swollen granules are to disintegrate; a reduction in breakdown suggests an increase of shear resistance of starch granules.

Table 1.2 Description of RVA pasting properties of starch

Parameter	**Description**
Pasting temperature	The temperature at which rapid viscosity increase begins
Peak viscosity	The maximum viscosity achieved
Hot paste viscosity (trough)	The minimum viscosity just before or after the system begins to cool due to disintegration of the swollen granules under slight shear (stirring) of the instrument
Final viscosity	The viscosity when the temperature of the paste reaches 50°C
Breakdown	The difference between peak viscosity and trough viscosity.
Setback	The difference between the final viscosity and the trough viscosity

Source: BeMiller (2011)

RVA has been used to calculate the relative degree of cross-linking of modified starches (Chatakanonda, Varavinit, & Chinachoti, 2000; Kaur, Singh, & Singh, 2006). Other methods for the determination of degree of cross-linking include the use of spectrophotometric methods to determine the amount of reduced phosphomolybdic acid complex (Morrison, 1964; Whistler et al., 1964) and the determination of monostarch monophosphate and distarch monophosphate using ^{31}P NMR (Sang, Prakash, & Seib, 2007; Kasemsuwan & Jane, 1996; Zhao et al., 2015).

Dynamical rheology has also been used to determine the viscoelastic properties of starch gels and pastes (Biliaderis, 2009). Two independent dynamic moduli can be obtained from the dynamic measurements which describes the viscoelastic properties of starch gels and pastes. The shear storage/elastic module (G') describes the energy stored and subsequently released, and the loss/viscous module (G") describes the energy dissipated as heat (Keetels, van Vliet, & Walstra, 1996). The viscoelastic measurements can also be expressed in the form of complex modulus (G*; G*= G' + *i*G'') and loss tangent (tan δ; tan δ= G''/G') which express the total contribution of the dynamic moduli in the changes in viscoelastic character of the polymer network structure (Biliaderis, 2009).

1.7.3 Conventional methods for studying retrogradation.

Differential Scanning Calorimeter (DSC), Visco-Amylo-Graph, RVA, and dynamical rheology are common methods for studying retrogradation of starch (Russell, Berry, & Greenwell, 1989; Keetels, van Vliet, & Walstra, 1996; Jane et al., 1999; Biliaderis, 2009; and Jane, 2009). DSC is used to monitor changes of phase transitions through measuring energy changes when the starch paste is subjected to programmed heating and cooling (Wang et al., 2015). These changes are expressed in transition temperatures (onset, T_O; peak, T_P; and conclusion, T_C) and enthalpy change (ΔH) due to first order (melting and crystallization) and second order (glass) transition of starch (Biliaderis, 2009). The transition temperatures and enthalpy changes have been used to measure the rate of retrogradation and the effect of temperature cycling and isothermal temperature during retrogradation of starch pastes (Zhou et al., 2010; Jacobson & BeMiller, 1998).

Other methods to study starch retrogradation include measurement of turbidity at 700 nm (Gidley & Bulpin, 1989) or 640 nm (Jacobson et al., 1997; Fu & BeMiller, 2017) by UV/Vis spectrophotometer, FTIR, NIR, Raman spectroscopy, NMR, light scattering (Gidley & Bulpin, 1989; Foster & Sterman, 1956), X-ray diffraction, blue value determination, and resistance of

starch to hydrolysis (Wang et al., 2015). Measurements of absorbance at 640 nm indicate the reduction in transmitted light by the starch pastes with time of storage. The increase in the turbidity and reduction of the transmitted light have been associated with microstructural changes and molecular associations of the components of starch that occur during early stages of retrogradation (Jacobson et al., 1997).

1.8 Starch properties studied using high-throughput platform

Conventional methods used for studying hydrothermal transition properties of starch are reliable and reproducible; however, the large quantity of material needed, and their time-consuming protocol limit the incorporation of these techniques in high-throughput screening platforms.

The use of high-throughput techniques to characterize starch is not new; they have been used to characterize corn kernel composition and starch structure, but not starch hydrothermal transition properties. These methods involve a 96-well plate for the characterization of AM and AP using the iodine binding assay (Kaufman et al., 2015); microarrays to identify variation in starch structure (Tanackovic et al., 2016); analysis of starch fine structure by single kernel sampling and high performance size exclusion chromatography and fluorophore-assisted carbohydrate electrophoresis (Yao et al., 2002; and Chen & Bergman, 2007); prediction of kernel composition based on single kernel near infrared spectroscopy (Cogdill et al., 2004; Baye, Pearson, & Settles, 2006; Janni et al., 2008; Tallada, Palacios-Rojas, & Armstrong, 2009); and changes of the viscosity of digested starch dispersion using molecular rotors (Lee, Ramer, & Toppozada, 2010).

Hydrothermal transition properties of starch in a high-throughput platform have not been studied. However, devices for the study of microrheology have been developed. Passive and active microrheology techniques assure the study of viscoelastic properties at microscopic level (Yang et al., 2017). Active microrheology can be achieved by Atomic Force Microscopy (Kuribayashi-Shigetomi et al., 2015), magnetic tweezers, and optical tweezers (Tassieri, 2019; Yang, et al., 2017). Passive microrheology is performed by laser interferometry (MacKintosh & Schmidt, 1999), video microscopy combined with diffusing-wave spectroscopy (Breedveld & Pine, 2003), and light scattering particle (Yang et al., 2017). Moreover, measurement of rheological properties can

be achieved by using plungers in parallel to measure rheological properties in an array of samples (Mansky and Hajduk, 2004) and a microfluidic device (Schultz & Furst, 2011).

Until this report, starch microrheology has been reported using γ-dodecalactone combined with diffusing-wave spectroscopy (Heinemann et al., 2004), high-resolution ultrasonic spectroscopy (Lehmann, Kudryashov, & Buckin, 2004), and particle tracking microrheology using high resolution microscopy (Moschakis, 2013). The development of these methods shows the advance in technology for the study of such important properties in viscoelastic materials. However, the application of these techniques requires a high investment and training to use them in a high-throughput platform. To the best of our knowledge, none of these techniques were used to characterize starch hydrothermal transition properties in a high-throughput platform.

1.9 Single kernel sampling

Selection of desired plants with the desirable genetic, physical, and/or chemical trait has been used to select crops for ensuring food security. Chemical composition analysis of the plant material is the most widely accepted reference method for desired trait selection (Baye et al., 2006). These methods are destructive and require large amount of plant/seed material that is obtained from bulk sampling.

Expression of the desirable phenotype and genotype is not uniform in all seeds; for this reason, selections based on analysis of individual kernels are necessary to separate those with the desirable traits. Moreover, in plant breeding the material collected is scarce and it is important to have enough material to ensure that plants with the desirable phenotype and/or genotype are propagated in the new offspring. Single Kernel Sampling (SKS) requires/involves: the protection of post-sampling germination; more than 80% of the seeds sampled to maintain viability (Becker and Cope 2008); obtaining at least a minimum required sample amount; obtaining a useful amount of sample from a specific location on the seed; maintaining a particular throughput level for efficiency purposes; reducing or virtually eliminating contamination between samples; and allowing for the tracking of separate samples and their correlation to other samples in a group (Becker and Cope 2008).

1.9.1 Mechanical approach for individual kernel sampling

Earlier efforts to sample individual kernels from different botanical sources have used mechanical approaches and laser, and their use have been reported (Table 1.3).

Table 1.3 Mechanical approaches for sampling individual kernels

Method	**Reference**
Hand-held rotary grinder with a #105 Dremel grinding bit	Sangtong et al., 2001
Abrasive screen	Cope, Kurth, and Oldenburg, 2012
Rotary blade	Deppermann et al., 2008
Breaking of the seed using an applied force	Cope, Jaehnel, & Mongan, 2012
Broach mounted in a programmable slide	Deppermann, Zhang, and Hinchey, 2014
Cookie cutter	Martinant et al., 2015
Razor blade	Yao et al., 2002
Animal nail clipper and cigar-type multiple-blade cutter	Becker & Cope, 2008
Laser beam	Hannappel, 2011; Hannappel, 2013; Cope & Kurth, 2008; Cope, 2010; Cope, 2011; Abbas et al., 2011; Becker et al., 2014)

The pitfalls of mechanical approaches and laser beam to collect tissues form single kernels are due to the defects that occur during processing. Cracks and damage of kernel, high shear forces leading to the heating of sample, disruption of sample while collecting, and damage of kernel by direct heat are some of the disadvantages for the use of mechanical approaches in SKS. Furthermore, collection of multiple samples from the individual kernels is not possible. In addition, length, sharpened edge, and reusability of the device would determine size and quality of the specimen.

1.9.2 New mechanical approaches for single kernel sampling

New mechanical approaches and techniques for the extraction of hard tissue have been developed. Medical devices for bone examination and removal of hard tissues have been developed with the goal to obtain a high efficiency rate and efficacy during sample collection. Furthermore, these devices were designed for the reduction of shear force and increase of the success rate when collecting samples. Commercial medical devices are trephine bur (Abdulrazaq, Issa, & Abdulrazzak, 2015), biopsy punch, bone biopsy needles (Wu et al., 2008), ultrasonic

cutters (Mathieson et al., 2017), piezoelectric bone surgery tools (Hennet, 2015), and cold plasma cutter (Gutierrez et al., 2013).

Piezoelectric bone surgery uses a sharp (scalpels and scrapers), serrated (saw), or diamond-coated metallic tip that vibrates at high frequency producing small movements, ranging between 60 to 210 μm (Hennet, 2015). Applying light pressure while cutting, allows the user to cut hard tissue and has been demonstrated to produce less damage by heat (Labanca et al., 2008).
Cold plasma has been used recently as a tool in surgery of soft and hard tissue. It uses a flow of helium gas that is energized when in contact with an electrical-energized metal blade to produce a plasma stream for cutting. The plasma stream can be controlled trough the electrical power and flow rate of gas for hard tissue removal (Gutierrez et al., 2013).

1.10 Molecular rotors

Molecular rotors are a group of molecules that has the ability to display an internal rotation in the fluorescence excited state (Haidekker & Theodorakis, 2010). These molecules are part of twisted intramolecular charge-transfer complexes (Akers, 2004; Gulnov, Nemtseva, & Kratasyuk, 2016) and their sensitivity is based in the restriction of the internal rotation. An ideal molecular-rotor sensor will have a large Stokes shift, that is the difference in wavelength of excitation and emission maxima; high sensitivity to structural rigidity; high brightness; and no coupling of the response to other physical and chemical property such as polarity (Alhassawi, et al., 2018).

1.10.1 Mode of action

Molecular rotors are composed of three units: an electron donor unit, an electron receptor unit, and an electron-rich spacer unit that is composed of a network of alternative single and double bonds (Haidekker & Theodorakis, 2010). Deactivation of this molecule is regulated by two competing deexcitation states: locally excited state or planar configuration (LE) and twisted intramolecular charge transfer state or non-planar configuration (TICT) (Loutfy, 1986 ; Haidekker & Theodorakis, 2007). Molecular rotors can relax either through LE or TICT which is determined by the environmental viscosity, molecular crowding, polarity of the media, and free volume (Haidekker & Theodorakis, 2007). In the TICT, the molecule experiences an internal molecular rotation due to the transfer of electron from the electron donor unit to the electron acceptor unit (Haidekker & Theodorakis, 2010). Inhibition of the TICT pathway leads to a decrease in the non-

radiate decay rate and an enhancement of the quantum yield, that is the ratio of emitted photons to absorbed photon (Loutfy, 1986).

The relationship between quantum yield (ϕ) and system microviscosity (η_m) is expressed with the Forster-Hoffman theory: $\mathrm{Log}\,\phi = x\,(\mathrm{Log}\eta_m) + C$; where x and C are probe-dependent and temperature-dependent constants (Loutfy & Arnold, 1982; Loutfy, 1986; Haidekker et al., 2010). It has been proved that free volume is also determinant in the molecular rotor quantum yield and changes in the free volume of polymeric systems can be measured (Doolittle, 1952; Loutfy, 1986; Jee et al., 2009; Gavvala et al., 2013; Jee, Bae, & Lee, 2010; Lee et al., 2014; Alhassawi et al., 2018).

1.10.2 Application of molecular rotors in biological samples

Molecular rotors have been used to monitor aggregation and polymerization of macromolecules (Loutfy & Teegarden, 1983); monitor protein aggregation (Hawe, Filipe, & Jiskoot, 2010; Kung & Reed, 1989; Sawada et al., 1992); examination of phospholipids bilayers and cell membrane (Nipper et al., 2008; Viriot et al., 1998; Haidekker, L'Heureux, & Frangos, 2000); and measurement of microviscosity and viscosity change in biofluid or live cells (Haidekker & Theodorakis, 2007; Haidekker et al., 2002; Haidekker et al., 2000). These show that application of molecular rotors in hydrophilic and hydrophobic environments is possible and subtle changes can be detected using molecular rotors.

1.10.3 Potential application of molecular rotors in food science

The application of molecular rotors in food industry is expanding. Molecular rotors have been used to sense changes in the rigidity of polymer films (Jee, Bae, & Lee, 2009; Jee, Bae, & Lee, 2010), to measure change of viscosity of enzymatic-digested starch paste in real time in a high-throughput way (Lee et. al., 2010), to study the free volume of different cyclodextrins (Gavvala et al., 2013), and to study changes of microviscosity of gelatinized starch dispersions (Gulnov et al., 2016).

Conventional hydrophilic molecular rotors such as 9-(2-carboxy-2-cyanovinyl) julolidine (CCVJ) and 9-(2,2-dicyanovinyl) julolidine (DCVJ) are more extensively used (Gavvala, Satpathi, & Hazra, 2015). The application of these molecular rotors to study food properties is possible due to their ability to sense changes in molecular crowding; polarity of media; micro-viscosity of

hydrophilic and hydrophobic liquids and semi solids; aggregation of molecules and macromolecules; phase behavior and phase transitions of hydrophobic molecules; and fluid flow. (Gulnov et al., 2016; Lee, Ramer, & Toppozada, 2010; Alhassawi et al., 2018).

Molecular rotors can help to reveal local spatial restriction and free volume in starch gels. Starches with different AM and AP fine structure could form different micro- and nano- structures with varying free volume; thus, the effect of AP-fine structure of starch during gelatinization and retrogradation can be studied. Furthermore, the increase of molecular crowdedness by introduction of internal cross-linking, which will increase molecular weight of starch granules, can be detected through monitoring changes of fluorescence intensity of molecular rotors.

1.11 Experimental aims

Although methods to characterize starch structure using a high-throughput way have been developed. There is still the need to develop techniques to study and characterize starch granules from individual kernels based on their hydrothermal transition properties. Spectrophotometric analysis has been used to determine some hydrothermal transition properties in starch slurries, but their suitability as high-throughput technique has not been investigated. Furthermore, the successful development of new methods to study micro-structure based on the use of molecular rotors coupled with fluorescence microscopy, may increase the reliability of this technique for characterizing hydrothermal transition properties of starch.

Our overall goal is to develop high-throughput techniques for studying starch properties combined with single kernel sampling for the selection of corn kernels with desirable native starch properties. It is hypothesized that high-throughput spectrophotometric techniques combined with SKS can replace the use of conventional methods to measure starch properties and functionalities. To accomplish this objective, we proposed the following specific aims:

1. Evaluating medical devices to effectively extract endosperm tissue from corn kernels;
2. Identifying a high-throughput technique to study starch retrogradation at a milligram level;
3. Evaluating the use of molecular rotors to identify shear resistant-starch granules and use conventional methods to corroborate the results obtained using molecular rotors.

The results obtained from this work will offer a new strategy to study hydrothermal transitional properties of starch and help screen starch granules based on these properties. Furthermore, the identification of high-throughput techniques combined with single kernels

analysis would allow rapid selection of novel candidates (maize seeds) with desirable properties/functionalities. The identification of such starch granule attributes would enhance breeding techniques and improve maize hybrid development.

CHAPTER 2. MILLIGRAM CRUDE STARCH ISOLATION FROM INDIVUDUAL CORN KERNELS

2.1 Introduction

There is a growing demand for the detection of specific traits in corn starch that is leading corn breeders toward the research and development of new techniques of analysis. The use of breeding techniques and the development of new to techniques to modify the genetic information of corn kernels with varying levels of mutation assure the creation of corn kernels containing starch granules with novel properties.

Analysis of whole grain is still a widespread technique. However, bulk sampling does not allow identification of individual kernels that may have different composition (Dowell et al., 2002). In plant breeding, the plant material collected is scarce and it is important to keep the viability of the kernel for further analysis or propagation of the desirable trait. In addition, expression of the desirable phenotype and genotype is not uniform in all seeds.

Single Kernel Sampling (SKS) has been used for the selection of seeds of interest without reducing viability of the material sampled (Tallada, Palacios-Rojas, & Armstrong, 2009; Yao et al., 2002; Cogdill et al., 2004; Janni et al., 2008). Different mechanical approaches have been developed for the sampling of individual seed with the objective of maintain the viability of the kernel, obtain the useful amount of material, maintain a particular throughput level, and reduce contamination of samples (Becker & Cope 2008).

In previous efforts, many defects in kernels were found when using mechanical approaches: cracks and damage to the corn kernel caused by heat when using a #105 Dremel grinding bit (Sangtong et al. 2001), a rotary blade (Deppermann et al., 2008), and an abrasive screen (Cope, Kurth, & Oldenburg 2012); or a laser beam (Cope, 2010; Cope, 2011; Abbas et al., 2011; Hannappel 2011; Hannappel 2013; Becker et al., 2014); and cracks in the corn kernel when using a broach (Deppermann, Zhang, & Hinchey 2014), animal nail clipper (Becker & Cope, 2008), and a cookie cutter-like tool (Martinant et al. 2015). Although the use of these devices was successful for collecting samples of individual kernels in a high-throughput way, there have been recent advances in the development of equipment with high efficiency and efficacy to remove hard tissue, prompting their evaluation as tools in SKS.

Medical devices for bone examination and hard tissue extraction have been developed and designed to reduce heat by shear force and to increase success rate when cutting hard and soft tissue. Example of medical devices are the trephine bur (Abdulrazaq, Issa, & Abdulrazzak, 2015), biopsy punch, bone biopsy needles (Wu et al., 2008), ultrasonic cutters (Mathieson et al., 2017), piezoelectric bone surgery tools (Hennet, 2015), and the cold plasma cutter (Gutierrez et al., 2013). The use of these devices for SKS could better assure that collection of a good specimen with, reduced kernel damage during sampling, and multiple point sampling on a single kernel are possible.

Starch isolation is an important part of carbohydrate research. Obtaining high purity and sufficient quantities without modification to the starch granule are required for characterization, chemical modification, fermentation, and industrial application (Puchongkavarin, Varavinit, & Bergthaller, 2005). Wet-milling is the main industrial process to separate fractions of starch, protein, germ, and fiber from corn kernels (Ji, Seetharaman, & White, 2004; Eckhoff, et al. 1997). Furthermore, new methods for the isolation of starch using cellulase and protease have been developed to increase starch yield that can be obtained from corn kernels and cereal flours (Wang & Wang, 2004; Wang & Wang, 2001; Lumdubwong & Seib, 2000; Cameron & Wang, 2006).

In this study a method for the extraction of endosperm samples from individual corn kernels and crude starch isolation from endosperm samples is reported. Medical devices were used to sample single kernels and two method for the isolation of corn crude starch from endosperm samples were evaluated. The efficiency of using medical devices to collect endosperm samples, subjective analysis of kernel damage, germination rate of sampled kernels, throughput of each method, and crude starch yield obtained from endosperm sample are reported.

2.2 Materials and methods

2.2.1 Chemicals and Materials

An ear of yellow dent corn was obtained from Dr. Yao's collection. Single-edged carbon steel blades, trephine bur drill with a diameter of 2.3 mm, 1.5 mm drill bit, glass beads of 0.5 mm, 1.5 mL Eppendorf tubes, and reagent grade sodium metabisulfite were purchased from Fisher Scientific (Hanover Park, IL). Neutral protease from *Bacillus sp.* (> 16 KNPU/g) was purchased from Sigma (Sigma-Aldrich Corp.)

2.2.2 Single Kernel Sampling

2.2.2.1 Extraction of endosperm sample by mechanical approach: trephine bur and carbon steel blade

Endosperm samples were extracted from single corn kernel using three mechanical devices: carbon steel blade, 1.5 mm drill bit, and trephine bur. A total of 20 kernels were used per medical device.

For extraction of endosperm sample using a trephine bur and drill bit, a 6 mm benchtop variable-speed drill press was used (China). Corn kernel was fixed in a drill chuck, a multipoint fixing device; then the trephine bur or drill bit were coupled to the bench-top drill. The spindle speed was set at 150 – 170 RPM and a hole was bored in the corn kernel. Finally, an endosperm sample was collected in an Eppendorf tube. The procedure was repeated to collect multiple endosperm samples from the same corn kernel (Scheme 1).

Collection of endosperm tissue using carbon steel blade was performed as described in Yao et al., (2002). Endosperm tissue was removed from the crown of a single kernel using a carbon steel blade. The angle of cut was about 45º to avoid damage of the germ. Tissue sample was collected in an Eppendorf tube. The use of a carbon steel blade did not allow multiple-point sampling from single kernel.

The recovery rate and throughput were recorded for each mechanical approach. The recovery rate was defined as:

$$\frac{\text{weight of endosperm sample}}{(\text{weight of kernel before sampling} - \text{weight of kernel after sampling})} * 100$$

The throughput was recorded as the total time used to collect the entire endosperm sample of all corn kernels using a medical device.

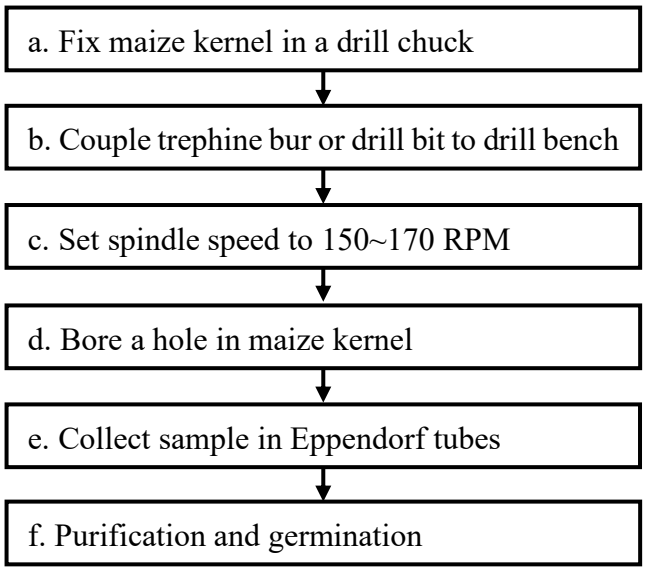

Scheme 2.1 Flow chart of the sample collection using two mechanical approaches

2.2.3 Crude starch isolation from endosperm sample.

Steeping method and a combination of sonication and protease digestion were compared for the isolation of crude starch from endosperm samples.

2.2.3.1 Steeping method

Steeping is the most widely used method available for isolation of crude starch from corn kernel. The method consisted of the following steps: addition of glass beads (0.5 mm diameter, 0.04 ~ 0.05 g) to each Eppendorf tube containing endosperm tissue; then, 200 µL of steeping solution (1% sodium metabisulfite solution (0.67% SO_2) was added and kept for 24 h with constant stirring at 100 RPM and 45 °C in a water bath. Afterwards, pericarp was removed manually. Centrifugation (2,000 × g, 5 min) was performed three times to wash the corn crude starch. After centrifugation, the supernatant was discarded, and the precipitate was dried out completely in an oven at 40 °C. The weight of each pellet was measured.

2.2.3.2 Sonication and protease digestion method

Sonication and protease digestion method was performed as per Cameron & Wang (2006). Endosperm sample was soaked with sodium phosphate buffer solution (0.1 M, pH 7.0). Neutral protease was added at 0.05% (w/w; endosperm base) and left for 4 hours in a water bath at 50 ºC

with constant stirring. Afterward, the tubes were transferred to an ultrasonic bath (40 KHz; Fisher Brand, USA) and applied ultrasonic treatment using a 100% amplitude for 30 min. After ultrasonication treatment, the corn crude starch was centrifuged at 100 RPM for 30 min and supernatant was discarded. Then, the corn crude starch was washed three times by centrifuging at 500 × g for 15 min and discarding the supernatant. Lastly, a final centrifugation at 3,000 × g for 15 min was performed to isolate crude starch.

2.2.4 Particle size

The method described by Yue Li et al. (2008) was used. A dispersion of isolated crude starch was prepared by mixing 5 mg of isolate with 1 mL of deionized water. The dispersion was stirred for 10 min. Then, a Mastersizer 2000 (Malvern Instruments, UK) was used to obtain the particle size data.

2.2.5 Microscope images

An inverted microscope (VWR, US) equipped with a Motic Cam Pro 252A (Motic; British Columbia, Canada) was used to collect images of corn starch. Isolated crude starch was dispersed at 0.01% in deionized water and placed in a microscope slide. The specimen was observed using magnification of 10 – 40X. Microscopic images were taken using the software provided with the Motic Cam Pro 252A.

2.2.6 Germination test.

Twenty sampled kernels using each mechanical approach were used for germination testing. Kernels were placed in a petri dish that contained a wet towel paper and the dishes placed in a dark room at 25 °C. The paper towel was watered every day with a garden sprayer to keep high humidity. After 2, 5, and 7 days, the germinated seeds were counted, and germination rate calculated as:

$$\left(\frac{\text{number of germinated seeds}}{\text{total number of seeds}}\right) * 100$$

2.2.7 Statistical Analysis

All experiments were performed in triplicate. Means and standard deviations were obtained using Microsoft Excel ver. 16.24 (California, USA).

2.3 Results and discussion

2.3.1 Evaluation of mechanical approach as a method for single kernel sampling

Table 2.1 Comparison of endosperm sample recovery, throughput, and germination rate of different mechanical devices used for sampling of individual corn kernel

Mechanical device	**Recovery rate (%)**	**Germination rate (%)**	**Throughput (kernels/day)**	**Scalability**
Drill bit	34.8 ± 20.2	85	~80 (10 kernels/hr.)	Yes
Trephine bur	88.6 ± 10.3	95	~100 (14 kernels/hr.)	Yes
Steel blade	98.7 ± 1.1	65	~200 (26 kernels/hr.)	No

The efficiency of each device is shown in Table 2.1. The recovery rate is the amount of endosperm sample recovered after extraction of the endosperm sample. A high recovery rate, 98.7%, was registered when a steel blade was used. Using the trephine bur a recovery rate of 88.6% was recorded. This device allows the collection of a good specimen. However, a ~12% endosperm sample was expected to be lost due to the ~0.3 mm wall that the device has. The use of the drill bit to collect sample form the corn kernel resulted in a low recovery rate. A drill bit produces a lot of debris and collection of endosperm tissues using this device was cumbersome.

The throughput for endosperm collection was recorded for each medical device and was in the following order steel blade>trephine bur>drill bit. The use of a steel blade resulted in rapid processing of kernels per hour, 26 kernels/hour. A short amount of time was used to align the kernel and cut the endosperm sample from the crown. The use of a trephine bur increased the time needed to collect the endosperm sample, 14 kernels/hour. The corn kernel needed to be fixed in a multiple-point fixing device and more time was needed for this step (Figure 2.1b). Moreover, the use of the trephine bur allowed multiple point sampling of the kernel increasing the amount of sample collected. The use of a drill bit was more cumbersome. The time needed to bore a hole in the endosperm was similar to trephine bur device. Although this device also allowed multiple point sampling, the production of small debris increased the time required to collect endosperm tissue.

2.3.2 Vitality of kernel after SKS

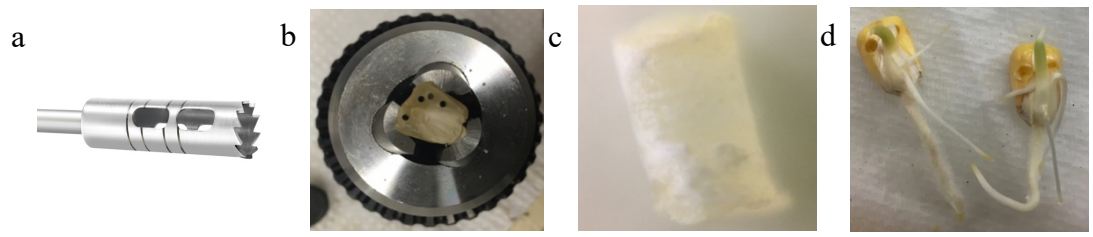

Figure 2.1 Depiction of a) trephine bur, b) multiple sampling point in corn kernel using trephine bur, c) cylindrical-shape endosperm sample obtained using trephine bur, and d) germinate kernel

Germination rate of sampled corn kernels using different medical devices are shown in Table 2.1. The highest germination rate of sampled corn kernel was for trephine bur (95%) followed by sampled corn kernel using drill bit resulted, 85%. This high germination rate was expected because the germ can be easily identified and avoided when collecting the sample. The advantage of using these medical devices was that a multiple point sampling can be performed increasing the amount of sample collected resulting in a more representative sample (Figure 2.1). The germination rate for corn kernel sampled using a razor blade is less than 80%. The use of the razor blade allowed the rapid collection of endosperm sample. However, damage of the germ can be produced due to irregularity in the shape of the corn kernel and the steep cutting angle used.

2.3.3 Comparison of crude starch yield by two isolation methods.

Table 2.2 Crude starch yield from endosperm samples using two isolation methods

Mechanical approach	**Crude starch isolation method**	**Crude starch Yield (%)**
Trephine bur	Steeping	47.3 ± 3.3
Trephine bur	Sonication + protease	50.4 ± 2.8
Steel blade	Steeping	30.3 ± 8.6
Steel blade	Sonication + protease	37.1 ± 10.6

The mean crude starch yields isolated from endosperm samples using two methods are shown in Table 2.2. Crude starch yield obtained using steeping method and a combination of

protease digestion and sonication ranges from 30.3% to 50.4 %. These values are lower than those reported by Ji, Seetharaman, & White (2004). They reported a starch yield of up to 60% starch yield using the steeping in sodium metabisulfite method. Crude starch isolated using the combination of neutral protease digestion for 2 hours at 50 ºC and sonication for 30 min resulted in the highest yield of 50.4%. It was reported that a higher yield of 61.2 – 76.1% can be obtained when neutral protease from *Bacillus subtilis* and sonication are introduced during starch isolation (Cameron & Wang, 2006). The starch recovery in this study was lower than reported previously because corn crude starch was isolated from endosperm sample rather than cereal flour.

Crude starch isolated from endosperm samples obtained by razor blade using the steeping method resulted in the lowest starch yield, 30.3 %. The use of the sonication and protease method did not increase the crude starch yield. The sample collected with razor blade contained a high amount of pericarp, which increased the initial endosperm weight. Moreover, the sample collected with razor blade was bulky and could not be digested well by the protease. The use of a tissue homogenizer or micro-blender before steeping of the endosperm sample could increase crude starch yield.

A pitfall for the isolation of crude starch from endosperm samples using both mechanical approaches was starch loss during the washing step. During the washing step, protein, lipids, fiber, and starch particles are discarded with the supernatant. In order to reduce the amount of starch lost, a pre-treatment with cellulase can help to increase the effectiveness of the method. Cellulase and protease digestion may help to disintegrate the tissues that entrap starch, enhancing its removal from the endosperm sample (Yue Li et al., 2008).

2.3.4 Particle size distribution

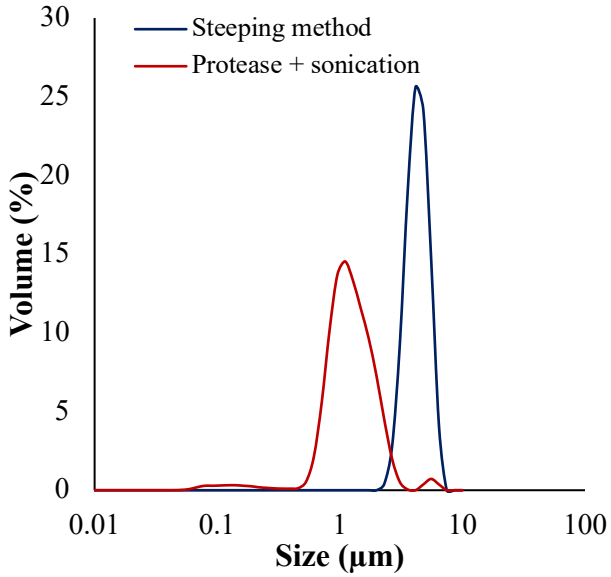

Figure 2.2 Distribution of particle sizes of corn crude starch isolated using two methods

Table 2.3 Particle size presented as volume percent of corn crude starch dispersions using two isolation methods

Method	Particle range (µm)		Average granule diameter (µm)	PdI*
	<1	>1		
Steeping method	0	100	4.3 ± 0.5	0.201 ± 0.128
Protease + sonication	35.21	64.79	0.8 ± 0.2	0.427 ± 0.183

* Polydispersity index value

The particle size distribution of crude starch dispersion isolated using steeping method showed a monomodal dispersion with a maximum peak at 4.15 µm. The volume fraction of starch granules using this method showed particles with size higher than 1 µm and average of 4.3 µm (Figure 2.2).

The use of the combination of protease digestion and sonication to isolate corn starch disrupted the corn crude starch into different fractions with different particle sizes. A trimodal

particle size dispersion was observed with maximum peaks at 0.14 µm, 1.1 µm, and 5.6 µm for the first, second, and third fraction, respectively (Figure 2.2). The use of protease digestion and sonication to isolate crude starch resulted in a reduction in particle sizes (average ~ 0.8 µm).

2.3.5 Microscope images of corn starch granules

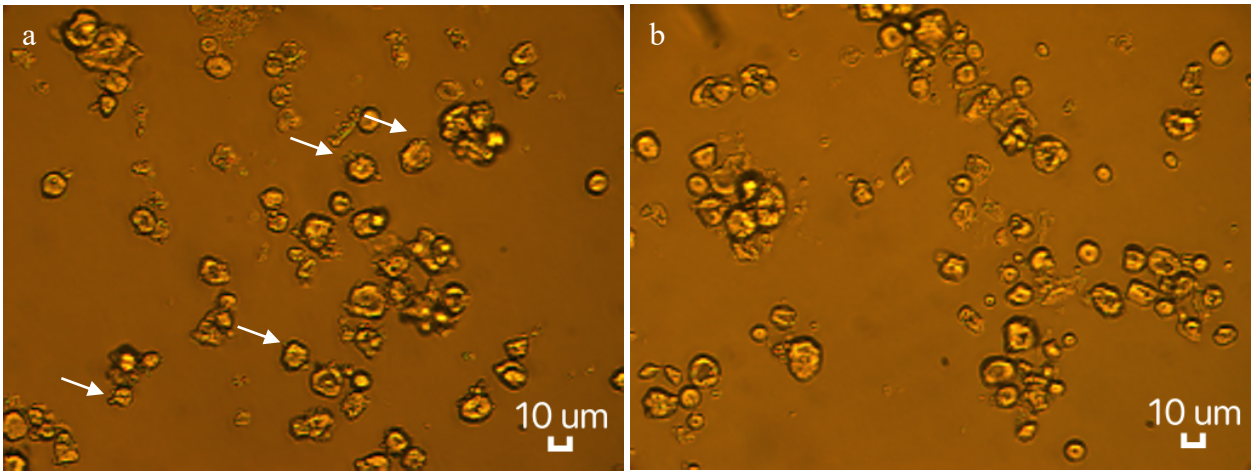

Figure 2.3 Microscope images of corn starch granules isolated by a) steeping method; and b) combination of protease digestion and sonication. Images were obtained using a magnification of 40 X

Microscope images of starch isolated using two methods are shown in Figure 2.3. Damage in the corn starch granules isolated using both methods was not observed. However, irregular shapes could be identified. It was observed a high number of small particles associated with the corn starch granule isolated using the steeping method (Figure 2.3a). It is likely that these small particles may have affected the particle size distribution. Association of small particles with starch granule isolated with protease digestion and sonicaion was not observed using a light microscope. However, small particles with diameter of ~1 µm were observed.

2.4 Conclusions

Two single kernel sampling methods were tested for the extraction of endosperm samples. A higher throughput was recorded when a razor blade was used. However, the damage inflicted to the kernel with the razor blade to the kernel resulted in a lower germination rate. The best mechanical approach to collect endosperm samples from single kernels in this report was using a

trephine bur. Although the throughput of the method was low compared to razor blade, is still a rapid approach for endosperm collection and is scalable.

Two methods for the isolation of crude starch from the endosperm samples was tested. Corn crude starch was isolated from endosperm sample after protease digestion at 50 ºC for 2 hours with constant stirring followed of a sonication with 100% amplitude for 30 min. The combination of extraction of endosperm sample using a trephine bur and crude starch isolation using protease and sonication resulted in a crude starch yield of about 50% which is higher compared to the steeping method in sodium bisulfate solution.

CHAPTER 3. STARCH RETROGRADATION AT MILLIGRAM LEVEL OF COMMERCIALLY AVAILABLE CORN STARCH

3.1 Introduction

Starch is added to food product as a functional ingredient. However, properties and functionalities of native starch varies with botanical source and within botanical source. In order to fulfill this demand, native starch is often altered or mixed with additives that will impact their properties and functionalities in food systems which can influence costumer acceptability (Silverio et al., 2000; Vamadevan & Bertoft, 2018).

The potential application of new commercial starches can be improved not only with chemical modification but also using biological modifications, i.e. mutation, or the combination of both chemical and biological modifications (Bemiller, 1997). The use of new methods to increase genetic variation in maize exponentially increases the number of potential individuals to be screened for starch properties.

Conventional techniques to study starch properties are difficult to incorporate in high-throughput screening platforms due to large amount of material needed and their time-consuming protocols. Several attempts have been made to use high-throughput techniques to characterize corn kernel composition and starch structure characterization (Kaufman et al., 2015; Tanackovic et al., 2016; Yao et al., 2002; Chen & Bergman, 2007; Cogdill et al., 2004; Baye, Pearson, & Settles, 2006; Janni et al., 2008; Tallada, Palacios-Rojas, & Armstrong, 2009); and viscosity of starch pastes (Lee, Ramer, & Toppozada, 2010; Gulnov et al. 2016). There is still the need to identify a technique that is sensitive to changes at milligram levels and provides characterization of starch properties with high reproducibility in a high-throughput platform.

Starch, a porous semi-crystalline and water-insoluble granule, is composed of two α-D-glucan components, amylose (AM) and amylopectin (AP) (Matignon & Tecante, 2017). When heated in presence of water the starch granule gelatinize and undergoes a series of changes including melting of crystallites, swollen of the granule, solubility, viscosity development, and disruption of intermolecular bonds of starch molecules (Biliaderis, 2009). After gelatinization, a reorganization of AM and AP into a water-insoluble semi-crystalline structure has been recorded in a process known as retrogradation.

Recrystallization of AM and AP molecules is described as a three-step process which include formation of critical nuclei (nucleation), growth of crystals from the nuclei formed (propagation), and continuous slow growth or crystal perfection (maturation) (Zhou et al., 2010). The rate of retrogradation can be accelerated by cycling the temperature of storage between temperature of nucleation and temperature of propagation. (Jacobson & BeMiller, 1998; Silverio et al., 2000; Zhou et al., 2010). Cycling the temperature of storage of paste between -20 ºC and 30 ºC has been demonstrated to be an efficient method to study retrogradation in a short period of time (Jacobson & BeMiller, 1998).

Retrogradation and other rheological characteristics of starch pastes can be studied using established conventional methods. Differential Scanning Calorimeter (DSC), Visco-Amylo-Graph, rapid viscosity analyzer (RVA), and dynamical rheology are the most common methods to study retrogradation of starch (Russell, Berry, & Greenwell, 1989; Keetels, van Vliet, & Walstra, 1996; Jane et al., 1999; Biliaderis, 2009; and Jane, 2009). Other methods include measurement of turbidity at 700 nm (Gidley & Bulpin, 1989) or 640 nm (Jacobson, Obanni, & Bemiller, 1997; Fu & BeMiller, 2017) by UV/Vis spectrophotometer, FTIR, NIR, Raman spectroscopy, NMR, light scattering (Foster & Sterman, 1956; Gidley & Bulpin, 1989) blue value determination, and resistance of starch to hydrolysis (Wang et al., 2015). Most of these methods, although reliable and reproducible, require substantial amounts of material and their time-consuming protocols limit their use in a high-throughput setting.

New techniques for the study of changes in micro-environment of biological systems using molecular rotors have been developed (Akers, 2004; Haidekker et al., 2002; Haidekker et al. 2002; Gulnov et al., 2016). Molecular rotor, such as 9-(2-carboxy-2-cyanovinyl) julolidine (CCVJ), is a fluorescent probe composed of an electron donor, electron receptor, and a π-conjugation system (Haidekker & Theodorakis, 2010). It deactivates its excited state through two complementary decays: a radiative decay or emission of fluorescence, called locally excited state (LE); and a non-radiative decay or release of heat without emission of photons and internal rotation, called twisted intramolecular charge transfer state (TICT) (Loutfy, 1986).

The TICT state is the main deactivation pathway of the molecular rotor. If the molecular rotor is an micro-environment with high viscosity or spatial restriction, the TICT pathway is hindered and more photons are released through LE (Akers, 2004; Gulnov et al., 2016). The extent of these changes can be monitored through the measurement of the quantum yield, the ratio of the

photons emitted to the absorbed photons. Although, the viscosity-sense property of the molecular rotor is the most used, it has been proved that free volume and mechanical properties of the medium are also determinant in the molecular rotor quantum yield (Doolittle, 1952; Loutfy, 1986; Gavvala et al., 2013, Jee, Bae, & Lee, 2009; Jee, Bae, & Lee 2010).

In this study a high-throughput technique to study starch retrogradation at milligram levels of starch is reported. Moreover, a method for the preparation of milligram-level starch pastes and a method for the measurement of accelerated retrogradation are also presented. A high-throughput platform using a single kernel analysis would allow rapid selection of novel candidates (maize seeds) with retrogradation-resistant corn starch. The identification of such starch granule attribute would enhance breeding techniques and improve maize hybrid development.

3.2 Materials and methods

3.2.1 Chemicals and materials

Commercially available normal corn starch (NCS) (Melojel) and waxy corn starch (WCS) (Amioca) were purchased from Ingredion. Reagent grade CCVJ, Na_2HPO_4 and NaH_2PO_4, propylene oxide (PO), acetone, sodium sulfate, sulfuric acid (H_2SO_4), deuterium oxide (D_2O), and dimethyl sulfoxide (DMSO) were purchased from Sigma (St. Louis, MO USA).

3.2.2 Preparation of chemically modified normal corn starch and chemically modified waxy corn starch

Hydroxypropylated starch was prepared using commercial NCS and commercial WCS based in the previous work of Fu & BeMiller (2017). Briefly, a 35% (w/v) starch slurry was prepared in 0.527 m sodium sulfate solution, and pH adjusted to 11.3. Propylene oxide (PO) was added to the starch slurry at ratio of 10%, 20%, and 40% of the dry base of starch. The mixture was kept at 25 ºC for 30 hours and constant agitation. Later, the starch slurry was neutralized with 1M HCl, washed twice with 50% acetone (three times the original volume), and once (one volume) time with 100% acetone. The granular modified starch was air dried at room temperature.

3.2.3 Analysis of hydroxypropylated starch

Molar substitution (MS) was determined by 1D ^1H NMR. A 10% dispersion of hydroxypropylated starch was prepared in 0.5 M H_2SO_4. The acidic dispersion was heated in a

boiling water bath for 1.5 hours and neutralized using 5 M NaOH, followed by freeze-drying to obtain sample hydrolysates.

The freeze-dried sample was dissolved in D_2O at 10 mg/ml. Two D_2O exchanges were performed by keeping sample in a boiling water bath for 1 hour followed by freeze-drying. After second exchange, freeze dried sample was dispersed in D_2O at 10 mg/ml, then 0.7 mL was transferred to a 5 mm Thin Wall Precision NMR sample tube. All the 1D ^1H NMR measurements were performed with a Bruker AVANCE DRX 500 spectrometer operating at 500 MHz. 1D ^1H NMR spectra were measured at 343 K with 32 scans, relaxation delay of 2 s between scans and an acquisition time of 2 s. All the spectra were processed using MestReNova version 10.0.2 (MestRelab Research, Spain). Chemical shift was referenced by water, and its chemical shift was calculated according to equation $\delta(H2O) = 7.83 - T/96.9$, where T is the absolute temperature in Kelvin (Jacobsen, 2007).

MS was calculated by the equations: $A/3 \div (B - A)/7$, where A is the area of the integrated 1D ^1H NMR spectrum around 1.2 ppm (3 methyl protons of the hydroxypropyl group) and B is the area of the spectrum in the range 3.1 - 4.1 ppm (4 glucosyl ring protons and 2 methylene + 1 methyne protons of the hydroxypropyl group) (Fu & BeMiller, 2017).

3.2.4 Preparation of starch paste using standard methods

Native and modified starches were used to prepare 0.125%, 3% and 5% (w/v) dispersions. For turbidity analysis and rheological measurements, dispersions were prepared in an RVA aluminum canister using deionized water. For fluorescence intensity analysis, sodium phosphate buffer (0.010 M and pH 6.9) containing CCVJ (5 μM) was used. Each starch dispersion was gelatinized in an RVA using standard protocol. An aliquot of 100 mg of the paste was transferred to a well of a clear-bottom 96-well black microplate. The microplate was stored at 4 ºC for further analysis.

3.2.5 Preparation of starch pastes at milligram level

Native and modified starches were prepared in a low-concentration dispersion at 0.1%, 0.5%, and 1% (w/v) in phosphate buffer (0.010 M and pH 6.9) containing CCVJ (10 μM) or degassed and deionized water, for fluorescence emission or turbidity determination, respectively. Dispersions were prepared in 10 mL tubes; then an aliquot of 200-uL was transferred to a well of

PCR microplate. Starch paste was prepared by atmospheric cooking in a water bath: first, sample was heated at 50 ºC for 15 min and then mixed by inversion of microplate; then, microplate was heated at 75 ºC for 15 min and mixing by inversion; lastly, microplate was heated at 95 ºC for 15 min and stabilized to room temperature. Thereafter, a 100 µL aliquot of each starch paste was transferred to a well of a clear-bottom 96-well black microplate. PCR oil (75 µL) was added to each well and microplate was covered with an adhesive film.

3.2.6 Rheological measurements

After preparation of samples using standard method (RVA), the 3% (w/v) paste was allowed to stabilize at room temperature. Then, aliquots of the NCS and WCS 3% paste were transferred to plastic reservoirs and sealed with plastic film to avoid water evaporation. The container with starch pastes were kept undisturbed in a refrigerated room at 4 ºC. After 1, 3, 4, 6, and 14 days, the retrograded starch paste was equilibrated to room temperature.

Dynamic viscoelasticity measurements was done as per Qiu et al. (2015). Briefly, an aliquot of the starch paste was placed in a HR3 Discovery Hybrid Rheometer (TA Instruments) and held for 3 min at 25 °C. The viscoelastic properties in the low-concentration starch paste was conducted by small amplitude oscillatory measurements using a cone plate geometry system (40 mm diameter, 2° cone angle, and truncation gap of 60 µm gap) (Biliaderis & Zawistowski, 1990). A strain sweep ranging from 0.01% to 200% at a fixed frequency (10 rad/s) was performed to stablish the linear viscoelastic regime. The frequency dependence viscoelastic moduli were measured by frequency sweeps between 0.1 and 40 rad/s within the linear viscoelastic domain at 0.5% oscillatory strain. Before each experiment, a thin layer of mineral oil was applied to each well of the microplate to prevent moisture evaporation.

3.2.7 Turbidity measurements

The method developed by Jacobson, Obanni, and Bemiller (1997), and Fu and BeMiller (2017) was used with some modifications. After 1, 2, 4, 6, 8 ,10, 12, 14, 16, and 18 day of storage at 4 ºC, microplates were stabilized at room temperature for 30 min and turbidity of starch pastes was obtained by measuring the absorbance at 640 nm in a Synergy H1 spectrophotometer (Biotek, Winooski, VT, USA) at 25 ºC. Water was used as blank.

3.2.8 Fluorescence intensity profiles of low-concentration starch pastes at milligram level by molecular rotor.

3.2.8.1 Preparation of CCVJ solutions

A stock solution was prepared by dissolving CCVJ in DMSO (100 mM). Then, aliquots of stock solution were dissolved in sodium phosphate buffer (0.01M, pH 6.9) to obtain a 5 μM and 10 μM solutions. A preliminary study of the effect of concentration of molecular rotor in the fluorescence intensity of CCVJ in different concentration of starch pastes revealed a linear relationship. In this study no more than 10 μM CCVJ was used to avoid molecular quenching of the fluorescent probe.

3.2.8.2 Fluorescence intensity measurement

Fluorescence intensity of CCVJ was measured in a Synergy H1 spectrophotometer (Biotek, Winooski, VT, USA) at 25 ºC and gain of 75%. The wavelength of maximum absorption (440 nm) was obtained from the excitation spectrum measured from 380 to 480 nm with a bandwidth of 2 nm. The wavelength of maximum emission was obtained from the emission spectrum measured from 460 to 540 nm with a bandwidth of 2 nm and an excitation wavelength of 440 nm. The Stokes shift was recorded during the time of the experiment and no significant change was observed.

3.2.9 Accelerated retrogradation by freeze-thaw cycling, temperature cycling and isothermal treatment.

Two freeze/thaw cycles (FTC) (first FTC, -20 ºC for 1 hour and 30 ºC for 1 hour; and second FTC: -20 ºC for 1 day and 30 ºC for 1 day); two temperature cycles (TC) (first TC, 4 ºC for 1 hour and 30 ºC for 1 hour; second TC, 4 ºC for 1 day and 30 ºC for 1 day); and two isothermal temperature (4 ºC and -20 ºC, measurements made at 1, 5, 10, 14 days of storage) where tested to determine the best method to accelerate retrogradation that could be incorporated in a high-throughput screening platform. From the preliminary test, the use of six FTC resulted in the best combination to accelerate retrogradation. Microplates containing low-concentration starch paste prepared at 0.1, 0.5, and 1% (w/v) of the modified and unmodified WCS starch paste were subjected to six FTC. Turbidity and fluorescence intensity were measured after each FTC. In this report, the results of the 1% starch pastes are shown.

3.2.10 Statistical Analysis

All experiments were performed in triplicate. Means and standard deviations were obtained using Microsoft Excel ver. 16.24 (California, USA).

3.3 Results and discussion

3.3.1 Characterization of chemically modified normal corn and waxy corn starch

Table 3.1 Modified WCS and NCS with different levels of propylene oxide and molar substitution

Sample	**Propylene oxide (%)**	**Molar substitution (n=2)**
Waxy corn starch	10	0.0348
Waxy corn starch	20	0.1043
Waxy corn starch	40	0.3224
Normal corn starch	10	0.0287
Normal corn starch	20	0.0680
Normal corn starch	40	0.2874

Native NCS and native WCS were modified with different amounts of PO and the molar substitution (MS) of each derivatized starch was obtained by NMR spectroscopy (Table 3.1). The MS expresses the number moles of hydroxypropyl groups introduced per mol of glucose (BeMiller & Whistler, 2009). An increase in the MS of hydroxypopylated starches was recorded when amount of PO used is increased. Similar results were observed by Liu, Ramsden, & Corke, (1999) and Han & BeMiller (2005); it was suggested that the leached molecules from NCS resulted in higher MS than the granular NCS molecule resulting in a decrease of the average MS of the NCS granule.

3.3.2 Evolution of dynamic viscoelastic moduli of stored starch pastes

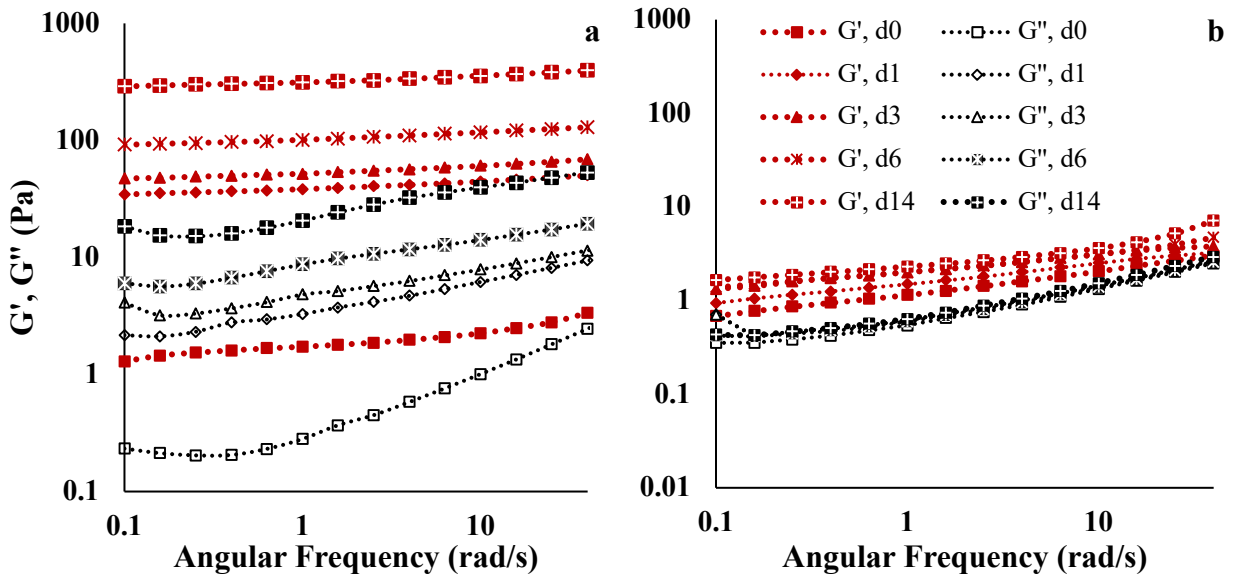

Figure 3.1 Evolution of viscoelastic moduli spectra, elastic/storage (G') and viscous/loss (G'') moduli, of normal corn starch (a) and waxy corn starch (b) pastes stored at different time intervals at 4 ºC. Viscoelastic moduli spectra were obtained by frequency sweeps at 25 ºC from 0.1 rad/s to 10 rad/s in the linear viscoelastic region

The evolution of the mechanical spectra during storage was recorded for WCS and NCS pastes prepared at 3% (w/v) starch concentration. The linear viscoelastic region was observed for both starch pastes when oscillation strain was applied from 0.01% to 10% (not shown). After such oscillation strain, a nonlinear viscoelastic region was observed.

Frequency sweep of WCS and NCS pastes stored at different time intervals at 4 ºC were recorded from of 0.1 rad/s to 40 rad/s at 0.5% oscillation strain in the linear viscoelastic range (Figure 3.1). Values of storage modulus and (G') and loss modulus (G'') was smaller in WCS pastes than in NCS pastes. The G' is a measurement of the elastic component of the paste; in other words, an increase of the G' will result from the development of a stiffer network; whereas the G'', is an indicator of the viscous properties of the material and estimates the energy dissipated as heat per cycle of deformation (Biliaderis, 2009).

It was observed that G' and G'' values increased with increasing angular frequency in stored pastes made of both starches. The increment in G' values with increasing angular frequency indicated more pronounced entanglements in the starch system. Furthermore, the mechanical

spectrum of both moduli increased with storage time at refrigeration temperatures which is attributed to an increment of entanglements/crystallization of the components in the gel network (Clark & Ross-Murphy, 1987). The contribution of the AM and AP reorganization in the retrograded starch paste is believed to contribute to the stiffness of the paste as result of the increase in the storage modulus.

3.3.3 Evolution of viscoelastic moduli during storage of starch pastes

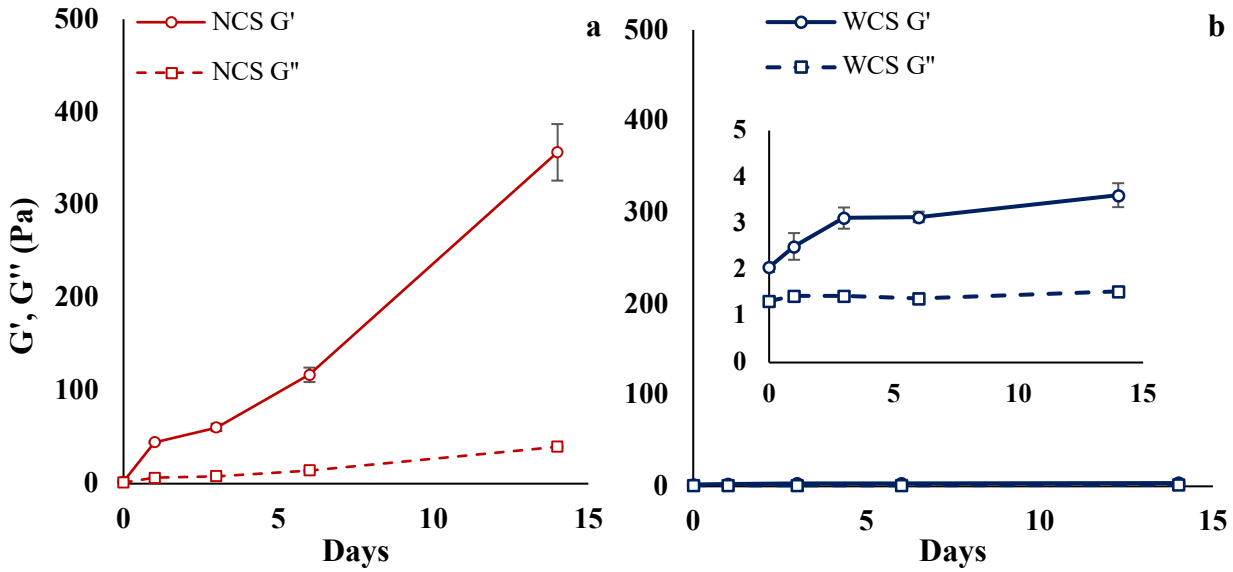

Figure 3.2 Development of elastic/storage (G') and viscous/loss (G'') moduli of normal corn starch (a) and waxy corn starch (b) pastes stored at different time intervals at 4 ºC. Evolution of storage and loss moduli were obtained at 10 rad/sec and 0.5% oscillatory strain

In the quick-cooled NCS pastes, the initial values of G' were higher compared to WCS paste (Figure 3.2). Thereafter, G' developed very rapidly from day 0 until day 1; then, a slow increase until day 3 and a rapid increase of the G' values until day 14 was observed (Figure 3.2a). Positive changes in G' values could be the result of an increase of the stiffness and number of entanglements of the paste when stored at refrigeration temperatures. The rapid increase of G' from day 0 to day 1 could be related to very rapid retrogradation (short-range), presumably AM-AM interaction, the slow increase in of G' from day 1 to day 3 may be an indicator of total retrogradation of AM (loss of networked AM) and retrogradation of AP; lastly, changes from day 3 to 14 could be related to stiffness of the network due to, possibly AM-AP interaction and AP-

AP interaction (Biliaderis & Zawistowski, 1990; and Fu & BeMiller, 2017). Moreover, other physical changes such as syneresis (Hoover et al., 2010) may have increased the stiffness of the retrograded paste.

Figure 3.2b shows the evolution of G' and G'' of WCS paste stored at 4 ºC. From the development of G' values, it was observed that retrogradation of WCS was a slow process compared to retrogradation of NCS paste. A slow and constant increase of G' values from day 0 to day 14 was recorded. It has been reported that commercially available waxy starches could be contaminated with up to 1% NCS granules (Jacobson et al., 1997), which may affect the molecular composition of the starch paste. The initial slightly increase of the G' values may be due to rapid AM retrogradation; thereafter, the increase of the G' values were presumably due to the recrystallization of AP molecules that increased the rigidity of the system. In order to register a major contribution of AP entanglements in the effect of G' values a higher concentration of AP is needed, 10% to 20% (Ring, 1987; and Ring et al., 1987).

For both starches the initial development of G'' values were very low and constant. For NCS, after day 3 there was a slight increase in the rate of development of G'' which may be related to the development of rapidly relaxing or weak interactions of AM and AP molecules. For WCS, the devolvement of G'' was small. The evolution of G'' in both starches may confirm the solid-like behavior of the retrograded starch paste.

3.3.4 Turbidity measurements of retrograded starch pastes

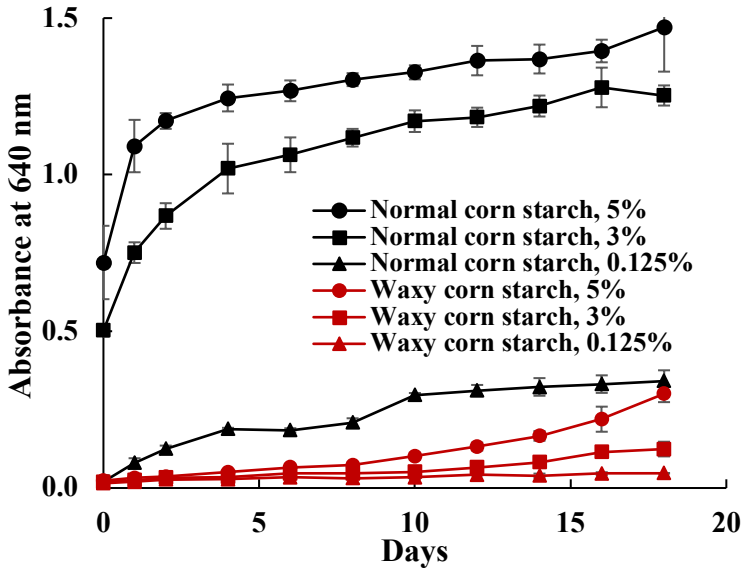

Figure 3.3 Absorbance at 640 nm of retrograded pastes of WCS (red lines) and NCS (black lines) at 0.125% (filled triangles), 3% (filled squares) and 5% (filled circles) w/v. Measurements were obtained at 25 ºC from pastes stored at different time intervals at 4 ºC

Aqueous dispersion of unmodified commercially available WCS and NCS starch were subjected to RVA using standard conditions for gelatinization and pasting. Thereafter, starch pastes were stored at 4 ºC to induce retrogradation. The absolute change in turbidity, absorbance at 640 nm, for each starch paste was obtained for each retrograded starch paste (Figure 3.3).

The turbidity profiles of each type of starch paste increased with the concentration of starch in the paste. NCS at 5% showed the highest initial turbidity among all the different concentrations for both starch pastes. For NCS pastes prepared at 3 and 5%, a rapid development of turbidity was registered during the first 4 days of storage (Figure 3.3). At the same time, the development of turbidity was of slower rate for the NCS paste prepared at 0.125%. After the 4th day of storage, the development of turbidity of all concentrations of NCS paste was of lower rate. A plateau in the turbidity development was registered for NCS prepared at 0.125% after 10 days of storage. No plateau was recorded for the retrograded NCS pastes prepared at 3% and 5% during the time of this experiment. Similar results were observed for Jacobson et al., (1997); and Fu & BeMiller, (2017).

Fu & BeMiller, (2017) reported that 3 main times could be observed based on the change of slope in the turbidity curves in NCS pastes prepared at 0.125%: the first at day 0, which correspond to short-term retrogradation; the second at day 2, that is the end of the process of short-term retrogradation; and day 6, which correspond to the end of long-term retrogradation. The same 3 times were observed in in this experiment.

The absorbance at 640 nm of WCS paste was very low at the beginning of the experiment and the rate of turbidity development was slow compared to NCS (Figure 3.3). Jacobson et al., (1997) reported a rapid development of turbidity in the first day of storage at 4 ºC of a 2% WCS paste and attributed it to small contamination of NCS in the commercial WCS. In this report, the development of turbidity of WCS pastes prepared from 0.125% to 5% was slow and constant.

During storage of AP-starch pastes prepared at 0.125% and 3% for 18 days at 4 ºC, the changes these pastes undergo were very little and the measurement of turbidity did not give any clue about the short-term and long-term retrogradation, i.e. reorganization of AP chains. Moreover, using a microscope technique, Jacobson et al. (1997) did not observe any visible structural change that could explain the slow increase in turbidity for retrograded WCS pastes at 2%. An increase in the absorbance at 640 nm was registered after day 10 in WCS paste prepared at 5%. Biliaderis, (2009) reported that the number of AP entanglements increases with an increase in the concentration of AP-containing starch pastes, which may contribute to the development of turbidity. In this study, a higher concentration of starch in the paste was not reported, because the scope of the study was to measure retrogradation in low-concentration, low-volume systems.

3.3.5 Fluorescence intensity profiles of retrograded starch pastes

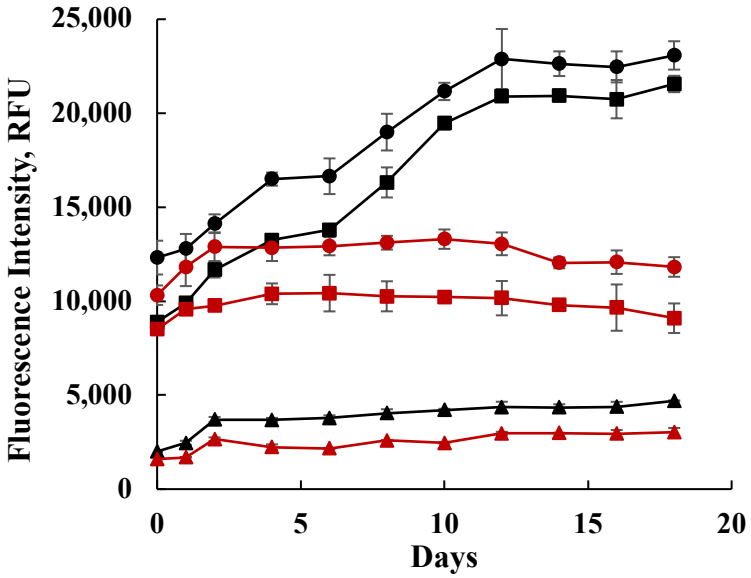

Figure 3.4 Development of fluorescence intensity of CCVJ in retrograded pastes of WCS (red lines) and NCS (black lines) at 0.125% (filled triangles), 3% (filled squares) and 5% (filled circles) w/v. Measurements were obtained at 25 ºC from pastes stored at different time intervals at 4 ºC

Fluorescence intensity of CCVJ was measured in retrograded starch pastes prepared at different concentrations (Figure 3.4). For this purpose, starch dispersions were prepared with phosphate buffer containing the molecular rotor and subjected to heat and shear in an RVA using standard conditions. Aliquots of 100 µL were transferred to a well of a clear-bottom black microplate and subjected to constant treatment at 4 ºC.

In this study, a molecular rotor was able to detect structural changes during retrogradation of NCS pastes prepared from 0.125% to 5% w/v. For NCS pastes, the highest initial fluorescence emission of CCVJ was recorded in pastes prepared at 5% followed by NCS paste at 3%. The lowest initial fluorescence intensity of CCVJ resulted in NCS prepared at 0.125%. For retrograded 3% and 5% NCS pastes, a rapid development of fluorescence intensity from day 0 until day 4 was observed. The fluorescence intensity developed from day 4 to day 6 was small; thereafter, a rapid increase in the fluorescence intensity from day 6 to day 10 was recorded. After day 10, the change in fluorescence intensity of CCVJ was small and constant. For retrograded NCS paste prepared at

0.125%, a rapid increase from day 0 to day 2 was recorded. Afterwards, the change in fluorescence intensity was small and constant.

For WCS, the highest initial fluorescence intensity values were recorded in the highest concentration of WCS paste, 5%, followed by pastes prepared at 3% and 0.125%. However, changes in the fluorescence intensity of CCVJ in retrograded WCS paste were similar for all the concentrations. First, a rapid increase in the fluorescence intensity from day 0 to day 2 was recorded. Thereafter, the change in fluorescence intensity were small and constant from day 2 until day 10. After the 10^{th} day, a decrease in the fluorescence emission of CCVJ was recorded until the end of the experiment for both WCS pastes prepared at 3% and 5%. The fluorescence intensity in retrograded WCS paste prepared at 0.125% did not change.

The results obtained by mechanical approach and turbidity data may help to explain changes registered with fluorescence emission of CCVJ. In retrograded NCS pastes, the rapid retrogradation is characterized by the development of AM gels after heating and is responsible for the formation of a network (Jacobson et al., 1997), possibly with high number of "nano-structures" with different size, which is affected by concentration of AM molecules in the paste. This could be observed in the initial fluorescence emission of NCS prepared at different starch concentration.

From day 0 to day 2, the loss of the networked AM and the consequent AM reorganization (AM aggregates), and possible AP recrystallization may be responsible for the reduction of free volume in the "nano-structures" creating a stiffer gel and slowing down the TICT of CCVJ, which resulted in an increase in fluorescence intensity. From day 2 to day 4, the development of fluorescence intensity is presumably due to the loss of networked AM, the development of more AM aggregates, and the binding of granules remnants into AM and AM aggregates (Jacobson et al., 1997). The slow increase in the G' modulus (Figure 3.2a) during this time confirmed the increase of stiffness of the gel network.

From day 4 to day 6, presumably AP retrogradation and co-crystallization of AM-AP mainly may have further shrunk the gel and restricted TICT state of CCVJ. From day 6 to 10, the end of the long-term retrogradation, i.e. AP-AP interaction and AM-AP interaction (Ring et al., 1987); and development of a network with higher elastic component, i.e. rapid development of G' values (Figure 3.2a), may have resulted in the inability of CCVJ to relax through the TICT state and more relaxation through the emission of photons via fluorescence.

Other physical changes that occurs during the storage of NCS paste, such as syneresis and increase in the formation of B-type crystal polymorphs, may have affected the development of the more rigid structure, increased the crystallization rate and interaction of AM and AP molecules, and reduction of the size of the nano-structures. The slow-down and small decrease in the development of fluorescence intensity of CCVJ in NCS pastes at 3% and 5% after day 12, may be related to those physical changes. Haidekker & Theodorakis (2007) showed that TICT state of molecular rotors was increased when exposed to aqueous media.

Based on the general shape of fluorescence intensity of the retrograded WCS pastes, three main stages could be observed: the first, at the day 0; second at day 2, the time the slope changes and is similar to the increase in G' (Figure 3.2b); and third at day 10, which correspond to the change in slope and possibly completion of long-term retrogradation.

The initial fluorescence intensity recorded, day 0, was presumably due to swollen and loose granules remnants with large pore sizes that were unable to slow down the internal rotation of the CCVJ. The higher concentration of WCS in the paste increased granule remnants and reduced the pore size, which resulted in higher fluorescence intensity. The recrystallization of AP in the granule remnant at day 2, may have increased the local spatial restriction and reduced internal motion of CCVJ. After day 2, the increase in recrystallization of AP molecules may have resulted in diffusion of CCVJ molecules to the aqueous phase and the increase of the internal twisting reducing the fluorescence intensity of CCVJ. A longer storage of the WCS paste at 4 ºC may have resulted in the development of more B-type crystal polymorphs and more diffusion of the CCVJ molecules to the aqueous media which may have resulted in an increase of the average relaxion through TICT stage.

3.3.6 Correlation of fluorescence intensity measurements of molecular rotor and rheological measurements.

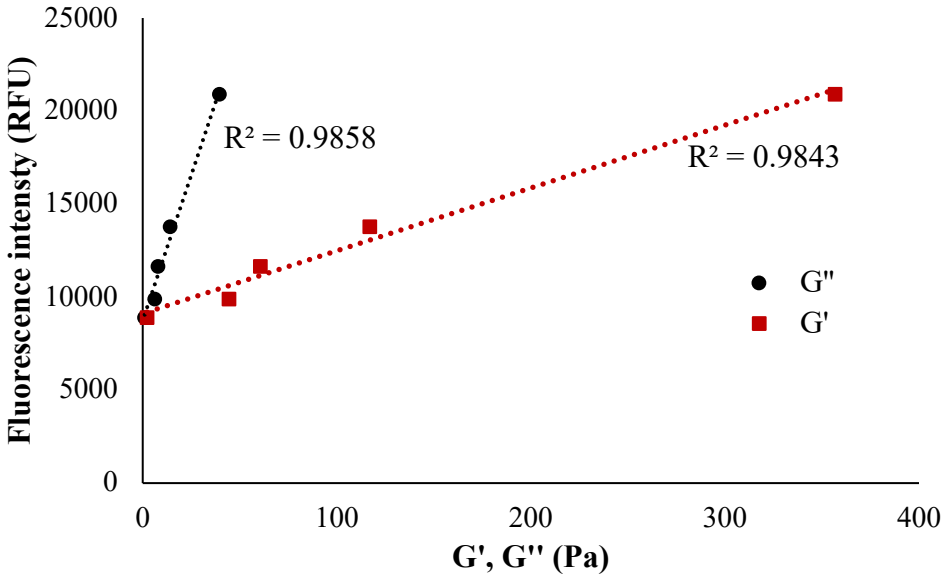

Figure 3.5 Correlation analysis of the evolution of storage (G'), loss (G'') moduli and fluorescence intensity of CCVJ in normal corn starch paste at 3% (w/v) with increasing storage time at 4 ºC. R^2 values are shown

The correlation analysis of the fluorescence emission of CCVJ and mechanical measurements of retrograded NCS paste are presented in Figure 3.5. It could be observed that there was a strong relationship between the storage and loss moduli and the fluorescence intensity in the retrograded paste (r=0.9921 and r=0.9928, respectively). The time dependent changes in the network of NCS pastes at 3 %, i.e. the devolvement of the entanglements in the retrograded paste with increasing storage at 4 ºC, resulted in an increase of the storage modulus and possible an increase in restricted space in the "nano-structures" which may have reduced internal twisting of CCVJ and increased the relaxation through photon emission.

Jee, Bae, & Lee (2009) reported that the reduction in the non-radiative decay channel, TICT, on 9-dicyanoviniljulolidine (DCVJ, analogue of CCVJ) depends not only on the free volume of the media but also on the elastic modulus (Young's modulus) of polymers. Moreover, Jee et al. (2010) obtained a positive correlation of the viscoelastic property, G', with reduction of internal motion of the molecular probe *trans*-4-[4-(dimethylamino)-styryl]-1-methylpyridinium iodide (4-DASPI). In addition to these findings, Gavvala et al. (2013) reported that quantum yield of DCVJ

increased in the following order α-cyclodextrin (CD)< β-CD < γ-CD. They reported that structure of γ-CD incorporated more than one molecular probe inside its cavity resulting in alteration of the excited state photophysics of molecular rotor, while the cavity of α -CD did not allow the accommodation of molecules of DCVJ.

The correlation analysis between the evolution of G', G'', and fluorescence intensity of CCVJ in the retrograded WCS paste showed R^2 values of 0.4815 and 0.1996, respectively, which resulted in a poor correlation (data not shown).

Gulnov et al. (2016) reported a poor correlation of microviscosity and macro-viscosity determined by fluorescence intensity of CVVJ and mechanical approach, respectively, in both potato starch pastes and gelatin gels prepared from 0.5% to 5%. They pointed out that some of the changes observed in the fluorescent intensity were due to the polymeric mesh formation in the potato and gelatin systems. A more detailed interpretation of the mechanical components, storage and loss moduli, in terms of the organization and interaction of AM and AP molecules during storage or thermal history, may have helped to explain the viscoelastic properties of the potato starch paste using molecular rotor.

3.3.7 Fluorescence intensity and turbidity profiles of retrograded hydroxypropylated starch pastes

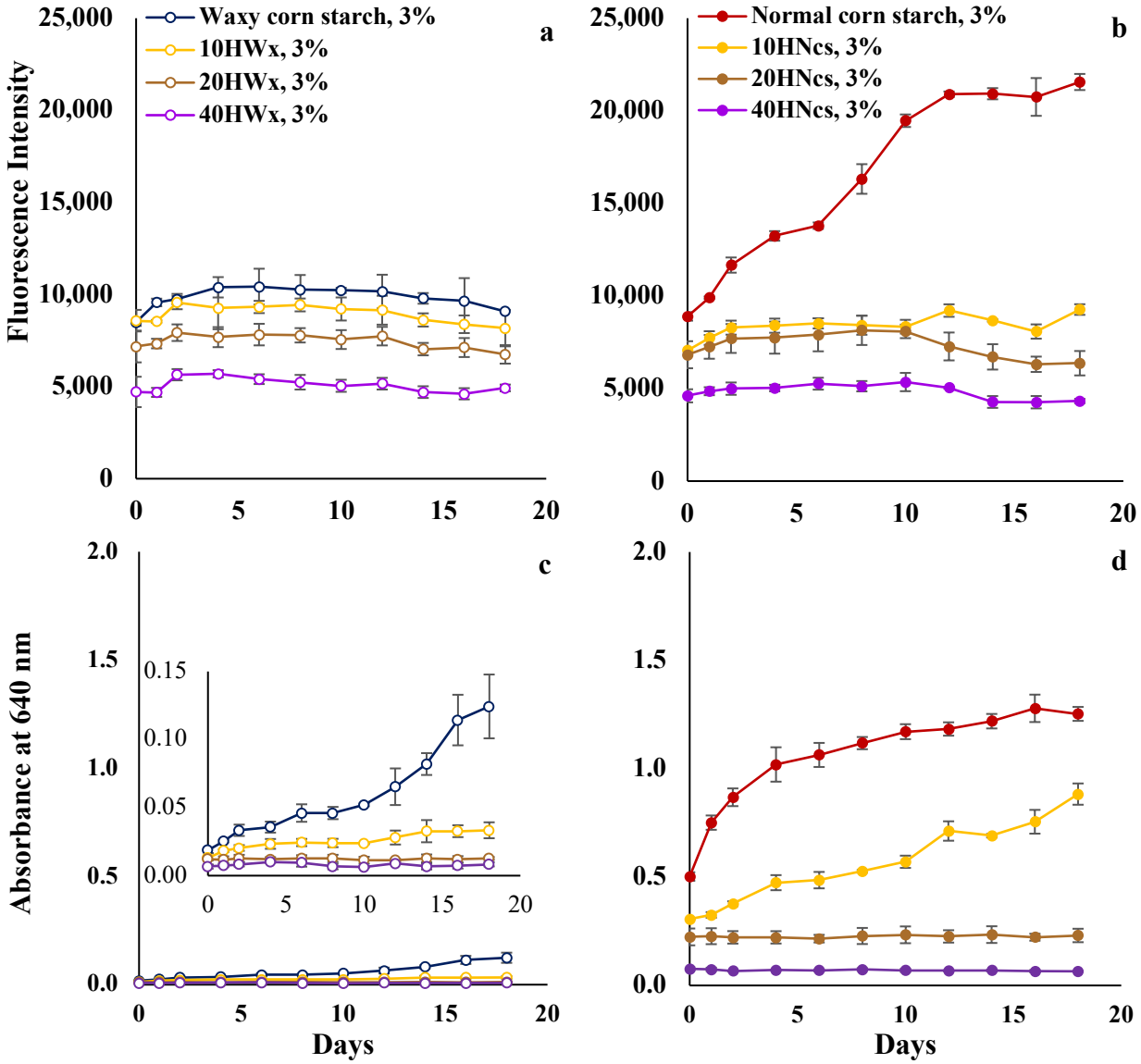

Figure 3.6 Development of fluorescence intensity of CCVJ (a and b) and turbidity (c and d) of retrograded native waxy corn starch, native normal corn starch, and hydroxypropylated starch pastes at 3% (w/v).Waxy corn starch and normal corn starch was reacted with 10% (10H), 20% (20H), and 40% (40H) propylene oxide (d.b.s.). Measurements were obtained at 25 ºC

The absolute changes in turbidity and fluorescence emission for each starch is presented in Figure 3.6. Changes in absorbance at 640 nm of hydroxypropylated WCS and NCS starches is shown in Figure 3.6c and 3.6d, respectively. In general, introduction of hydroxypropyl groups in

the WCS and NCS granule resulted in a stabilized material that developed turbidity at slower rate than native starch pastes. The initial turbidity, measured after gelatinization, decreased as the as the amount of hydroxypropyl groups increased in the native starch. Moreover, the turbidity development was of slower rate as the amount of hydroxypropyl groups was increased in the native starch. Both samples, WCS and NCS reacted with the highest amount of propylene oxide, underwent the least retrogradation during storage at 4 ºC.

The fluorescence intensity (FI) profiles for both modified starches are shown in Figure 3.6a and 3.6b. For modified NCS, it was observed that the initial (day 0) fluorescence intensity for the modified starches decreased as the amount of hydroxypropyl groups increased. Thereafter, an increase in the fluorescence intensity was observed until the second day of storage for all the hydroxypropylated NCS; then, a plateau was reached fast. Lastly, a decrease in the fluorescence intensity was observed after 10 days of storage at 4 ºC.

The fluorescence intensity profiles for modified WCS after day 0 were different to those of NCS. A small increase in the fluorescence intensity was recorded until the second day of storage. Afterwards, no significant change in the fluorescence intensity was recorded until the last day of storage at 4 °C.

Hydroxypropyl groups were introduced to the starch structure due to the ability to retard retrogradation in starch pastes. Hydroxypropyl groups introduce the capacity to form H-bonds in the starch paste network and reduce the recrystallization rate an interaction of both AM and AP molecules. However, it has been shown that CCVJ molecules has the affinity to form hydrogen bonding with the solvent or media; thus, increases the TICT formation (Haidekker & Theodorakis, 2007). In this study. it is not clear if the reduction in fluorescence intensity of CCVJ in hydroxypropylated starch pastes was the result of more hydrogen bonding due to presence of hydroxypropyl groups or reduction in the time-dependent changes of AM and AP. More detailed study needs to be done to elucidate these findings.

3.3.8 Accelerated retrogradation of low-concentration corn starches pastes by freeze-thaw cycles

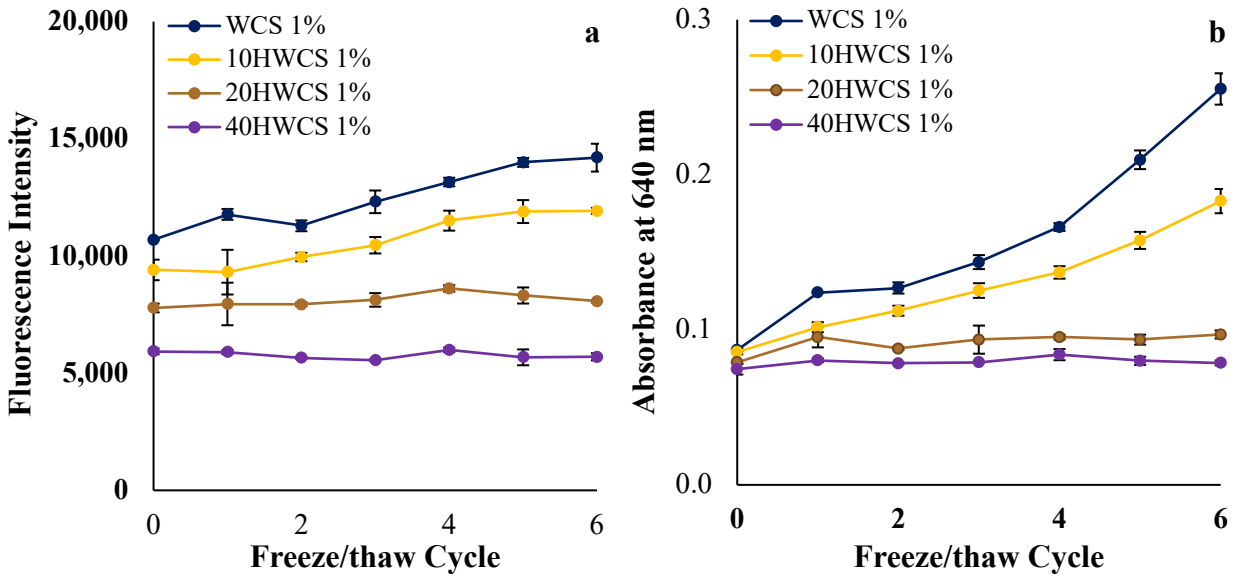

Figure 3.7 Development of fluorescence intensity of CCVJ (a) and absolute absorbance at 640 nm (b) of retrograded waxy corn starch and hydroxypropylated waxy corn starch prepared at a starch concentration of 1% w/v. Accelerated retrogradation was obtained by treating the starch paste with 6 freeze-thaw cycles (FTC). Each FTC consisted of storage of the paste at -20 ºC for 1 hour followed of storage at 30 ºC for 1 hour. Hydroxypropylated starch was prepared by reacting WCS with 10% (10H), 20% (20H), and 40% (40H) propylene oxide (d.b.s.). Measurements were carried out at 25 ºC

For this analysis, WCS was chosen to focus on the retrogradation behavior of AP, which is the responsible for slow retrogradation. Low-concentration starch pastes of modified and unmodified commercially available WCS were obtained by preparing pastes in PCR-microplates and subjected to atmospheric cooking. Pastes were prepared with deionized water or phosphate buffer containing the molecular rotor for turbidity and fluorescence intensity measurement, respectively. Aliquots of 100 µL were transferred to a well of a clear-bottom black 96-well microplate and subjected to constant treatment at 4 ºC. Six FTC were applied to accelerated retrogradation to each microplate. The development of turbidity and changes of fluorescence intensity of CCVJ were recorded to determine the best technique to detect changes during accelerated retrogradation of low-concentration WCS pastes. Furthermore, the effect of a retrogradation inhibitor was measured with both techniques (Figure 3.7).

For turbidity measurements, the retrogradation rate was decreased with increasing amount of the retrogradation inhibitor, hydroxypropyl groups. The least retrogradation rate or inhibition of retrogradation was observed in the sample containing the highest MS value. As shown in Figure 3.7b, the unmodified WCS paste showed the highest initial absorbance at 640 nm. There was a sharp increase in the turbidity developed after the 2nd FTC until the 6th FTC. At this point the highest absorbance at 640 nm was registered in the unmodified WCS.

Development of turbidity in a starch paste during retrogradation is associated to the number and size of molecular associations, and number of swollen granules remnants that can scatter light (Craig, Maningat, Seib, & Hoseney, 1989; and Jacobson & BeMiller, 1998). AM and AP recrystallization is a 3-step process that includes, nucleation, propagation, and maturation (Eerliengen et al., 1993). The first two are the more critical during the recrystallization process. Increasing the nucleation of the starch components will result in an increase in the retrogradation of starch. During FTC, Jacobson & BeMiller, (1998) showed that freezing starch pastes using a -15 ºC freezer, which has a slower freezing rate, resulted in more molecular associations due to the starch paste kept near the temperature of maximum nucleation. Afterwards, thawing of the frozen starch paste resulted in propagation and perfection of the crystallites. The rate of these two increases with increasing thawing temperature (Zhou et al., 2010).

The development of fluorescence intensity in the unmodified and modified WCS was slow and constant. The highest initial fluorescence intensity was recorded in the unmodified WCS (Figure 3.7a). An increase in the fluorescence intensity after the first FTC was recorded; then, a decrease in the emission of CCVJ. Thereafter, a slow and constant change in the fluorescence intensity was recorded until the 5th FTC. Subjecting the paste to next FTC resulted in a slower fluorescence intensity development. For modified WCS with 10% PO, the fluorescence intensity development was at slower rate than that of unmodified WCS and showed the plateau development after the 5th FTC. WCS with the highest MS value underwent the least retrogradation, obtained with turbidity measurements; and had the lowest fluorescence intensity development.

These results showed that measurement of fluorescence intensity development was capable of discriminate among retrograded starch pastes with different amount of hydroxypropyl groups. However, after subjecting the modified and unmodified WCS paste to FTC, the increase in fluorescence rate was slower than turbidity measurements.

3.4 Conclusions

Fluorescence intensity of CCVJ was used to measure changes of retrogradation of NCS and WCS pastes. The first part of the experiment was to correlate the development of fluorescence intensity of CCVJ with the development of the network in retrograded starch paste. It was determined that physical changes and development of structure during retrogradation of NCS pastes at the starch concentrations used affected emission of CCVJ and this was detected quantitatively. Time-dependent changes during storage at 4 ºC in the WCS paste suggested a diffusion of CCVJ to the aqueous phase and reduction of the fluorescence emission, higher internal twisting.

The second part of the experiment was to identify the best high-throughput technique to measure retrogradation of starch pastes prepared with mild shear. For this purpose, WCS paste was used to simplify the molecular organization and to identify the technique that can measure long-term retrogradation, AP recrystallization. Our results indicate the best method to identify rates of retrogradation of unmodified and modified AP-containing starches at milligram level was with the combination of accelerated retrogradation and turbidity measurements. Hydroxypropylated WCS was used due to the fact that hydroxypropyl groups inhibits retrogradation. However, the effect of the interaction of hydroxypropyl groups and CCVJ is not well understood and more detailed investigation will be needed to explain our experimental results.

CHAPTER 4. IDENTIFICATION OF SHEAR-RESISTANT STARCH AT MILLIGRAM LEVELS USING A MOLECULAR ROTOR

4.1 Introduction

Maize is one of the staple foods of humankind and one of the top sources of starch. The global grain market is expected to grow from $267 billion in 2017 to $352 billion in 2021 (Business Research Company, 2018). In 2012, corn was the source of 74% of starch for industrial use and its primary use was in the native form, followed by hydrolyzed and modified starches (Business Research Company, 2013). Application of native starch is diverse, not only for the food industry but also the paper, textiles, pharmacy, and chemical industries.

When subjected to heat in the presence of water, the starch granule undergoes a series of changes, and these hydrothermal transition properties confer a wide range of functionalities (BeMiller, 2019). Hydrothermal transition properties are responsible for food-industry relevant properties such as gelatinization, granule swelling, native crystalline melting, loss of birefringence, starch solubilization, pasting, and retrogradation (Sullivan & Johnson, 1964; BeMiller & Whistler, 2009; Biliaderis, 2009). Starch has two main components: amylose (AM) and amylopectin (AP). AM is a linear chain of glucose units linked by α-1,4 glycosidic bonds and contains limited ramifications in the α-1,6 position; whereas AP contains both glucose units linked by α-1,4 glycosidic linkages and a great number of glucose units linked by α-1,6 glycosidic bonds (BeMiller & Whistler, 2009).

Chemical, physical, and enzymatic modifications are introduced to native starches to enhance their properties and enable functionalities (BeMiller, 2019). Chemical cross-linking of starch granules introduces phosphate linkages which result in covalent bonding of starch components. As result, starch properties are affected and include restrict swelling, reduction of granule rupture, loss of viscosity, and formation of a stringy paste during cooking (Woo & Seib, 1997). Sodium trimetaphosphate (STMP) and phosphoryl chloride ($POCl_3$) are the most common cross-linker agents (Hirsch & Kokini, 2002) and no more than 1% of STMP and 0.1% $POCl_3$ (weight of dry starch) can be reacted with starch for food purpose (BeMiller & Whistler, 2009).

The most used conventional method for studying cross-linked starch is the rapid viscosity analyzer (RVA) which characterizes starch paste properties based on the measurement of viscosity and recording changes in viscosity during cycles of heating and cooling with constant stirring

(Wiesenborn et al., 1994). From the RVA profiles, several paste properties can be obtained, such as paste viscosity, paste temperature, hot paste viscosity, final viscosity, and breakdown. Breakdown is the difference between paste viscosity and hot paste viscosity. A reduction in the breakdown will be the result of an increase in the intra-molecular and inter-molecular bonding of the starch granule (Heo, Lee, & Chang, 2017). Furthermore, RVA has been used to calculate the relative degree of cross-linking of modified starches (Chatakanonda, Varavinit, & Chinachoti, 2000; Kaur, Singh, & Singh, 2006).

New techniques for the determination of changes in the microviscosity of biological systems have been reported. Molecular rotors, such as 9-(2-carboxy-2-cyanovinyl)-julolidine (CCVJ), are fluorescent molecules that relax from their excited state by two distinct states: locally excited state or planar configuration (LE) and twisted intramolecular charge transfer state or non-planar configuration (TICT) (Loutfy, 1986; Haidekker et al., 2002; Haidekker & Theodorakis, 2007). The rate of TICT relaxation is dependent of the microenvironment of the matrix. In a high viscosity environment, molecular crowding and polarity of the media restrict the formation of the TICT state resulting in more relaxation through LE (Akers, 2004; Alhassawi, et al., 2018).

One alternative to chemical modification is the identification of native starches with improved native-starch functionalities. Fine structure of AP; i.e. chain length, distribution of chain lengths, and ratio of short to long chains; AM structure; and AM-AP ratio can be affected by mutation of the starch biosynthetic enzymes (Vamadevan & Bertoft, 2018). Furthermore, new mutagenesis techniques of maize kernels were developed (Weil & Monde, 2007) which promotes changes in the maize genotype to increase source of variation and affect starch properties relevant to the food industry These new techniques provide the possibility for high numbers of mutants with starch having diverse properties and functionalities. However, the identification of individual kernels with desirable traits has two limitans: 1) the vitality of seed needs to be maintained, and 2) limited amount of material is available for analysis. High-through put techniques for the identification of starch properties and functionalities are necessary to identify novel mutant maize with native starch substituent.

The aim of this report was to use molecular rotor to detect level of disruption of starch granules after subjecting to shear forces. Measurements using conventional methods was used to corroborate the results obtained by measuring the signal of the fluorescent probe. For this purpose, native and cross-linked WCS are used as model samples. It is hypothesized that subtle changes in

the internal organization of the starch granule can be detected using the fluorescent emission of CCVJ.

4.2 Materials and methods

4.2.1 Chemicals and Materials

Commercially available waxy corn starch (Amioca, WCS), and ClearJel® were purchased from Ingredion. Reagent grade 9-(2-carboxy-2-cyaovinyl)-julolidine (CCVJ), sodium trimetaphosphate (STMP), phosphoryl chloride ($POCl_3$), deuterium oxide (D_2O), dimethyl sulfoxide (DMSO), and sodium sulfate were purchased from Sigma -Aldrich Corp. (Saint Louis, MO, US). Eppendorf tubes (1.5 mL) were purchased from Fisher Scientific (Hanover Park, IL, US). Clear-bottom 96-well black microplates were purchased from Greiner (Monroe, NC, US). Double-distilled water was freshly prepared whenever required.

4.2.2 Preparation of chemically modified waxy corn starch

The protocol for crosslinking of starch with STMP was obtained from Lim & Seib (1993) and Hirsch & Kokini (2002); and was used with some modifications. A 40% (w/w) starch dispersion was prepared in deionized water containing 2% sodium sulfate and the pH of the mixture was adjusted to 11 with 1M sodium hydroxide. After complete dispersion, 0.01%, 0.1%, 0.33%, and 1%, (d.b.s.) of STMP was added under constant stirring. Afterwards, the mixture was stirred for 3 hours at 40 ºC. The reaction was terminated by neutralizing the dispersion with 1M hydrochloric acid solution. The cross-linked WCS was recovered by centrifugation (3000 × g for 10 min), followed of 3 cycles of washing with deionized water and centrifugation. Finally, cross-linked WCS was dried at 40 °C.

Crosslinking with $POCl_3$ was performed as described by Gunaratne & Corke, (2007) with some modifications. A 40% (w/w) dispersion of starch (20 g, dry based) was prepared with deionized water containing 2% sodium sulfate and pH of the mixture was adjusted to 11.0 with 1M sodium hydroxide solution. Phosphoryl chloride was added at 0.01%, 0.033%, and 0.1% (d.b.s) to the starch dispersion. The mixture was stirred at 25 ºC for 1 hour; then, the starch slurry was neutralized with 1M hydrochloric acid solution. The cross-linked starch was recovered as explained before.

4.2.3 Paste properties, solubility, and shear resistance determination.

The protocol stablished by Peng & Yao (2018) was used to determine paste properties of native and modified starches. Briefly, starch material (1.5 g) was mixed with deionized water in an aluminum canister to make a 6% (w/w) starch slurry. A rapid viscosity analyzer (Newport Scientific, Australia) with the following heating and cooling conditions was used: 1) temperature held at 50ºC for 1 min, 2) increased to 95ºC at 12ºC/min and held at 95ºC for 2.5 min, and finally 3) temperature reduced to 50ºC at 12ºC/min and held at 50ºC for 2 min. Pasting properties of each starch sample were obtained from the RVA curve using Thermocline version 2.2 software.

4.2.4 Shear resistance determination by molecular rotor at microliter level.

4.2.4.1 Preparation of molecular rotor

A stock solution was prepared by dissolving CCVJ in DMSO (100 mM). Then, aliquots of stock solution were dissolved in sodium phosphate buffer (0.01M, pH 6.9) to obtain a 10 μM solution.

4.2.4.2 Preparation of low-concentration starch paste for measurement of fluorescence intensity

Native WCS and derivatives were used to prepare starch dispersions (0.5% and 1%; w/v)6 in sodium phosphate buffer containing the molecular rotor in 200 μL PCR tubes. Glass beads (100 mg, 0.5 mm diameter) were added to each starch dispersion. The starch dispersion was cooked in a water bath: the dispersion was heated at 50 °C, held for 15 min, and mixed by inversion; followed by heating at 75 °C, held for 15 min, and mixed by inversion; lastly, heated at 95 °C and held for 15 min. After heat treatment, dispersions were allowed to cool down to room temperature and shaken for 10 min at 3000 RPM in a Genie cell disruptor (Scientific Industries; Bohemia, US). An aliquot of 100 μL of each non-shaken and shaken sample was transferred to a well of a clear-bottom 96-well black microplate and allowed to stabilize overnight at room temperature.

4.2.4.3 Fluorescence Intensity measurement

Fluorescence emission spectra of CCVJ was measured with a Synergy H1 spectrophotometer (Biotek; Winooski, USA) at 25ºC and gain of 75%. The wavelength of maximum absorption (440 nm) was obtained from the excitation spectrum measured from 380 to 480 nm with a bandwidth of 2 nm. The wavelength of maximum emission was obtained from the

emission spectrum measured from 460 to 540 nm with a bandwidth of 2 nm and an excitation wavelength of 440 nm.

4.2.5 Microscope images

Microscope images were obtained using an inverted microscope (VWR; Illinois, US) equipped with a Motic Cam Pro 252 A (Motic, British Columbia, Canada) and the software Motic Image Plus 2.0 were used to record images. Aliquots from each sample was dispersed at 0.01% in deionized water, iodine solution was added, and placed in a microscope slide. Specimens were observed using magnification of 10X– 40X.

4.2.6 Statistical Analysis

All experiments were performed in triplicate. Analysis of variance (ANOVA) was performed with the R Studio program Version 1.1.463 (Boston, MA, USA).

4.3 Results and discussion

4.3.1 Preparation of chemically modified waxy corn starch

Table 4.1 Cross-linking condition to prepare cross-linked waxy corn starch using two cross-linker agents

Substituent (%, s.b.)	**Phosphorylation condition**			
	pH	**Temperature ºC**	**Time (h)**	**Sodium sulfate (%)**
STMP*				
0.01	11	40	3	2
0.1	11	40	3	2
0.33	11	40	3	2
1	11	40	3	2
$POCl_3$**				
0.01	11	25	1	2
0.033	11	25	1	2
0.1	11	25	1	2
ClearJel®				

*Sodium Trimetaphosphate

**Phosphorus oxychloride

Cross-linking of WCS in aqueous slurry has been carried out using two cross-linking agents. Table 4.1 shows the phosphorylation conditions for each cross-linker. A basic medium, pH 11,

and 2% sodium sulfate were kept constant during phosphorylation of WCS with both cross-linkers. Temperature and reaction time varied for each cross-linker used. Cross-linking with STMP was carried out at 40 ºC and kept mixing for 3 hours, while phosphorylation of WCS with $POCl_3$ was carried out at 25 ºC and constant mixing for 1 hour. The amount of cross-linker agent used in the reaction varied from 0.01% to 1% (s.b.) for STMP and 0.01% to 0.1% (s.b.) for $POCl_3$. Woo & Seib (2002) found that the amount of phosphate groups in the cross-linked WCS increased with higher amount of cross-linker used. Furthermore, an impact in the starch functionalities is expected with increasing amount of crosslinker. Hirsch & Kokini, (2002) reported that the swelling factor of modified WCS is greatly reduced by $POCl_3$ than STMP.

The reaction kinetics of each type of cross-linker is unique and the level and position of the substituent will determine physical properties and functionalities of the modified starch. Zhao et al. (2015) reported that the introduced phosphorus by cross-linking reaction of sweet potato starch with STMP resulted in the formation of monostarch monophosphate and distarch monophosphate in a molar ratio of 1:1.03. Similar results were reported by Sang, Prakash, & Seib (2007) by crosslinking wheat starch with a mixture of STMP/STPP (sodium tripolyphosphate). While phosphorylation with $POCl_3$ resulted in the formation of monostarch monophosphate only with AM in solution and a mixture of monostarch monophosphate and other types of phosphate ester in the insoluble fraction that contained AM and AP (Kasemsuwan & Jane, 1994).

4.3.2 Effect of cross-linking on pasting properties of waxy corn starch

The RVA profiles of unmodified WCS, ClearJel®, and cross-linked materials with STMP and $POCl_3$ at 6% (w/w) concentration are shown in Figures 4.1 and 4.2. Paste properties of the crosslinked samples are described in Tables 4.2 and 4.3.

4.3.2.1 Paste properties of cross-linked WCS with STMP

Table 4.2 Pasting parameters of native waxy corn starch, cross-linked waxy corn starch prepared with different levels of sodium trimetaphosphate (STMP), and ClearJel®, a commercially available shear-resistant starch. Similar letter means no significant difference (n=3)

Sample	Peak Time (min)	Pasting Temperature (ºC)	Paste Viscosity (cP)			
			Peak	Final	Breakdown	Setback
Native WCS	4.0±0.1^{d}	74.6±0.5^{bc}	1305±66.7 ^{abc}	912±33.6^{d}	462±18.4^{a}	69 ±17.5^{d}
WCS - 40	4.1±0.0^{d}	74.6±0.3^{bc}	1060 ±11.2^{d}	697±8.1^{e}	437.±24.7^{a}	94±6.4^{d}
WCS-STMP 0.01	4.0±0.1^{d}	73.6±0.4^{c}	1166±40.1^{cd}	1164 ±55.4^{c}	270±14.0^{b}	268±16.6^{c}
WCS -STMP 0.1	4.6±0.2^{c}	73.9±0.1^{bc}	1453 ±42.9^{a}	1712±73.9^{a}	117±27.2^{c}	376±14.9^{b}
WCS -STMP 0.33	4.6±0.1^{c}	74.5±0.5^{bc}	1251±28.8^{bc}	1642±21.7^{a}	75±28.2^{c}	466±28.6^{a}
WCS -STMP 1	6.9±0.1^{a}	75.1±0.4^{ab}	1024±30.8^{d}	1356±37.5^{b}	12 ±2.9 ^{d}	344±12.2^{b}
ClearJel®	5.6±0.2^{b}	76.3±0.8^{a}	1320±102.8^{ab}	1703 ±140.1^{a}	104±2.6^{c}	487 ±41.2^{a}

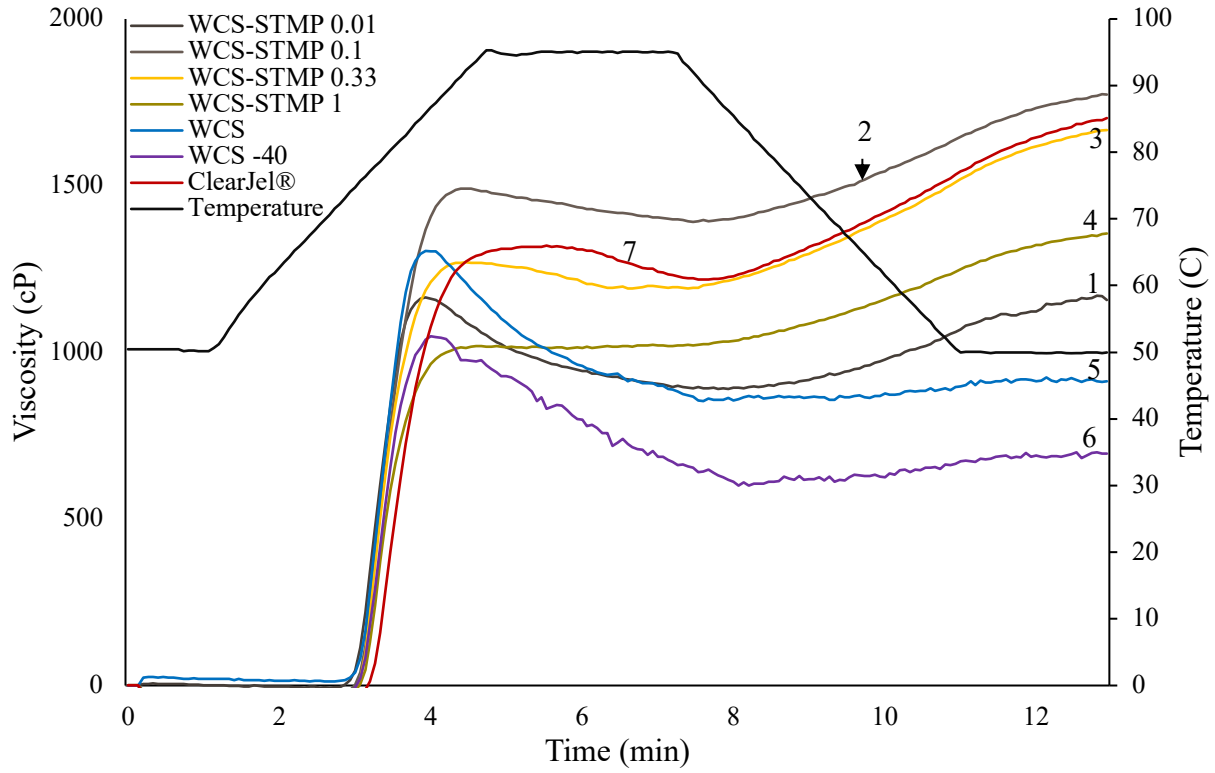

Figure 4.1 RVA profiles of 6% (w/w) of native corn starch and chemically modified starches. Waxy corn starch was reacted with sodium trimetaphosphate (STMP) at 0.01% (1), 0.1% (2), 0.33% (3), and 1% (4). Waxy corn starch (5), waxy corn starch treated with same conditions as cross-linked samples (WCS-40) (6), and a commercially available shear-resistant sample (ClearJel®) (7) are included for comparison

At this concentration, no significant difference in the peak time, pasting temperature, breakdown, and setback were observed between the unmodified WCS and the WCS treated with the same conditions as the cross-linked WCS (WCS-40) (Table 4.2). However, the peak viscosity and final viscosity were higher in the native WCS than the treated WCS. The WCS treated with similar cross-linking conditions has been kept for 3 hours at pH 11 and 40 ºC. After this treatment, a considerable number of starch granules were likely gelatinized due to the high pH. Consequently, a decrease in the final viscosity was recorded in the RVA profile.

It could be observed (Table 4.2) that small amounts of STMP, 0.01%, resulted in an increase of the final viscosity and setback compared to native WCS. However, a reduction in breakdown from 462 cP to 270 cP in the crosslinked sample with STMP at 0.01% was observed. Furthermore, increasing amount of reacted STMP up to 1%, a greater reduction of the breakdown was recorded. Similar results were reported by Heo, Lee, & Chang (2017). These results indicate that the increase in the cross-linked agent resulted in an increase of inter-bonding and intra-bonding resulting in a more ordered granule that can maintain their integrity (Jyothi, Moorthy, & Rajasekharan, 2006).

Increasing the amount of STMP reacted with WCS (i.e., >0.01%), increased the peak time from 4.0 min in the native WCS up to 6.9 min in the sample crosslinked with 1% STMP, and pasting temperature from 74.6 ºC in the native WCS up to 75.1 ºC in the sample crosslinked with 1% STMP. The increase of both pasting temperature and peak time indicate that more energy is required to break the new introduced chemical bonds in the granular starch (Wongsagonsup et al., 2014). In addition, the new bonds may have created a restriction to swelling, which enabled the granule to withstand high temperature, 95 ºC, and shear.

The WCS crosslinked with 0.1% of STMP showed the higher final viscosity and peak viscosity, 1712 cP and 1453 cP, respectively. Increasing the concentration of STMP, up to 1%, in the modified WCS resulted in a reduction of the final viscosity up to 1356 cP and the peak viscosity up to 1024 cP. The reduction of these paste properties with increasing amount of STMP could be attributed to a higher density of cross-linking and reduction of swelling behavior (Hirsch & Kokini, 2002). Moreover, the reduction of swelling behavior may have resulted in a granule with lower volume and solubility, and thus, a reduction in the peak viscosity.

4.3.2.2 Paste properties of cross-linked WCS with POCl3

Table 4.3 Pasting properties of native waxy corn starch, cross-linked waxy corn starch prepared with different levels of phosphorus oxychloride ($POCl_3$), and ClearJel®, a commercially available shear-resistant starch. Similar letter means no significant difference (n=3)

Sample	Peak Time (min)	Pasting Temperature (°C)	Paste Viscosity (cP)			
			Peak	Final	Breakdown	Setback
Native WCS	4.0±0.1^{d}	74.6±0.5^{b}	1305±66.7^{b}	912±33.6^{b}	462±18.4^{a}	69 ±17.5^{c}
WCS 25	4.0±0.1^{d}	74.1±0.1^{b}	1100±73.8^{c}	782±13.9^{b}	416±18.9^{b}	77 ±1.5^{c}
WCS -$POCl_3$ 0.01	4.3±0.1^{cd}	74.3±0.5^{b}	1555±59.7^{a}	1608 ±50.0^{a}	238 ±13.8^{c}	291 ±3.5^{b}
WCS -$POCl_3$ 0.033	4.5±0.1^{c}	74.3±0.5^{b}	1394±41.2^{b}	1733±48.6^{a}	143±15.9^{d}	482±13.2^{a}
WCS -$POCl_3$ 0.1	4.9±0.1^{b}	74.5±0.5^{b}	1302±26.9^{b}	1656±48.1^{a}	99±8.5^{e}	453±27.1^{a}
ClearJel®	5.6±0.2^{a}	76.3±0.8^{a}	1320±102.8^{ab}	1703 ±140.1^{a}	104±2.6^{de}	487 ±41.2^{a}

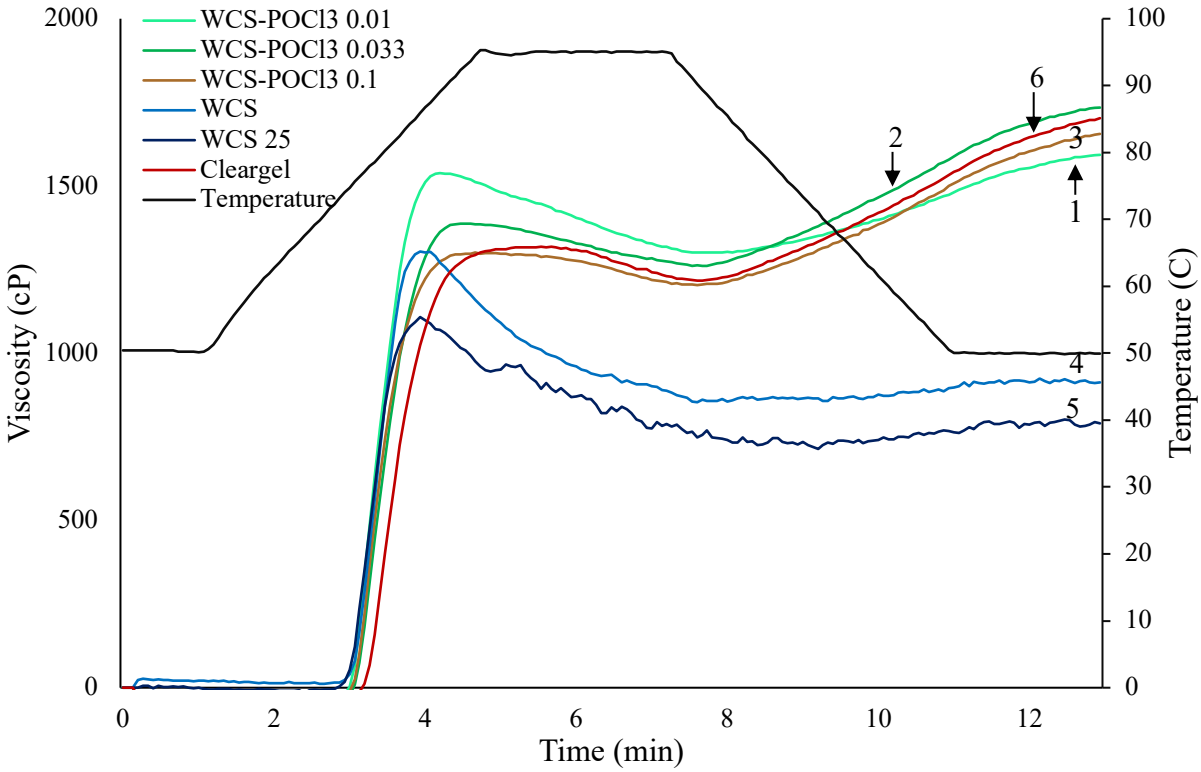

Figure 4.2 RVA profiles of 6% (w/w) d.b. of native corn starch and chemically modified starches. Waxy corn starch was reacted with phosphoryl chloride ($POCl_3$) at 0.01% (1), 0.033% (2), and 0.1% (3). Waxy corn starch (4), waxy corn starch treated with same conditions as cross-linked samples (WCS 25) (5), and a commercially available shear resistant sample (ClearJel®) (6) are included for comparison

For the WCS treated with similar condition as those crosslinked with $POCl_3$ (WCS 25), similar paste properties were observed compared to native WCS. However, a decrease in peak viscosity in the treated WCS was observed, possibly due to mild gelatinization of WCS granules treated at pH 11 and kept at 25 ºC with constant stirring for 1 hour. Addition of $POCl_3$ increased the peak time from 4 min to 4.9 min in the WCS reacted with the highest amount of $POCl_3$, 0.1%. As explained before, the increase of number of covalent bonds may have resulted in a granule that can withstand processing at higher temperature and more time needed to start the swelling of the granule. However, the pasting temperature was similar for all the modified and unmodified WCS, except for the commercially-available shear-resistant starch.

Small amount of cross-linker, 0.01% $POCl_3$, reacted with WCS increased the peak viscosity from 1305 cP in the native WCS to 1555 cP in the cross-linked WCS. This increase in the peak viscosity has been linked to a high degree of swelling that resulted in a strong interaction between starch granules (Hirsch & Kokini, 2002). The final viscosity was greater in the WCS cross-linked with any amount of $POCl_3$ compared to the native WCS. A decrease of the breakdown from 462 cP in the native WCS to 99 cP in the WCS crosslinked with the highest amount of $POCl_3$, 0.1%, was observed. Finally, the setback value increased in the cross-linked WCS with both 0.033% and 0.1% $POCl_3$ compared to the native WCS.

4.3.2.3 Paste properties of commercially-available shear-resistant starch

The commercially-available shear-resistant samples, ClearJel®, had peak viscosity, final viscosity, and breakdown values between cross-linked samples with 0.01% and 0.33% STMP. However, setback and pasting temperature values were higher in ClearJel® than all the STMP cross-linked WCS. Compared with cross-linked WCS with $POCl_3$, ClearJel®'s peak viscosity, final viscosity, breakdown and setback were similar to the samples cross-linked with 0.033% and 0.1% $POCl_3$. Lastly, ClearJel® showed high peak time and pasting temperature compared to samples crosslinked with any amount of $POCl_3$ and native WCS.

4.3.3 Light microscopy

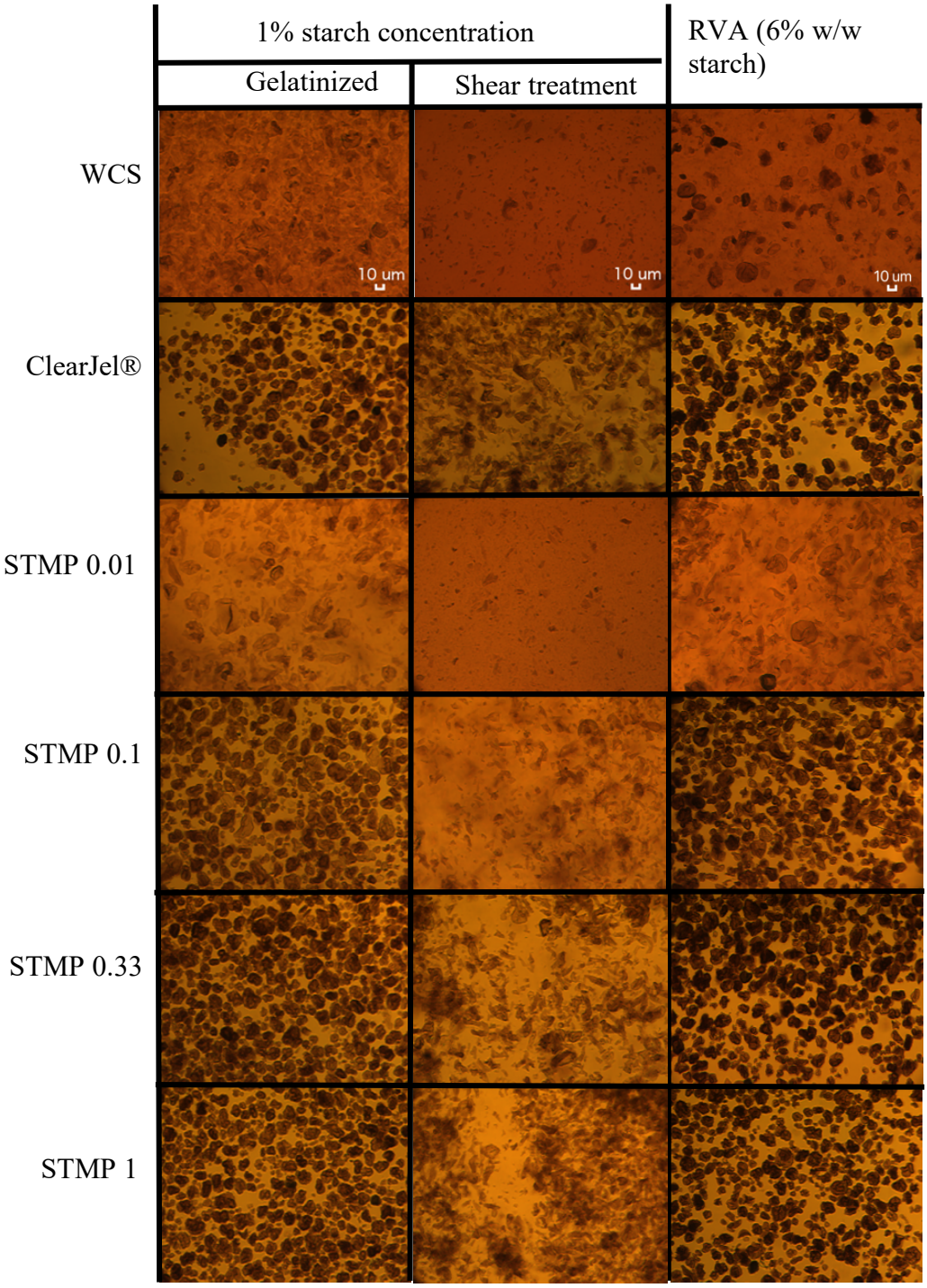

Figure 4.3 Micrographs of iodine-stained waxy corn starch, ClearJel®, and waxy corn starch crosslinked with different amounts of phosphoryl oxychloride ($POCl_3$) and sodium trimetaphosphate (STMP). Starch dispersions were shaken at 3000 RPM for 10 min. Images were taken with a magnification of 20X

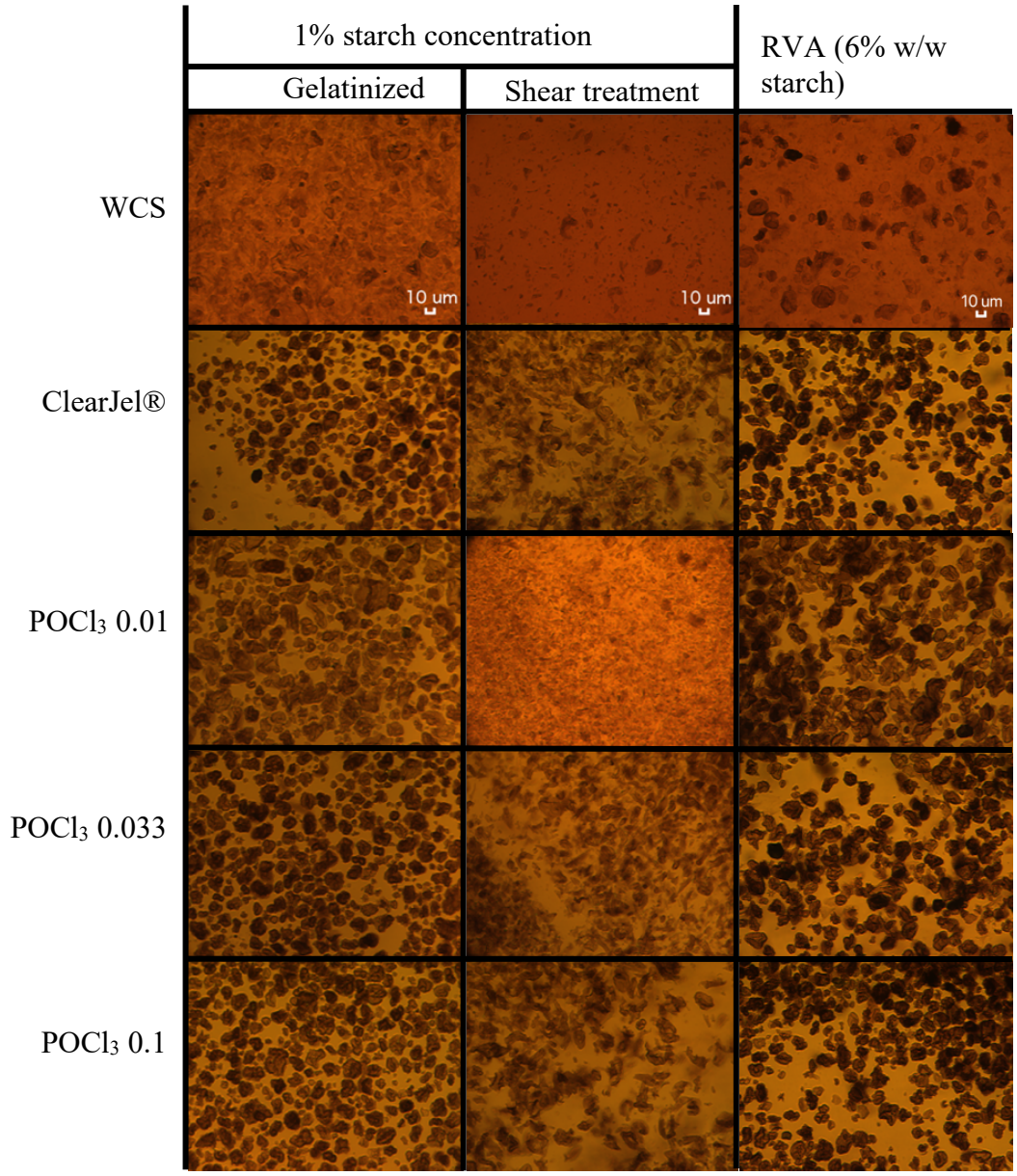

Figure 4.3 continued.

Microscope images from aliquots of the samples prepared using RVA and the samples prepared at low-concentration of starch are shown in Figure 4.3. It was observed that the native WCS experienced an irreversible swelling when heated, and disrupted granules and granule remnants could be observed when native WCS granules were heated for longer periods of time at 95 ºC. When shaken, the granules of gelatinized WCS were disrupted and most of the "ghost granules" disappeared and small granule remnants were visible.

WCS having lower amount of cross-linker, 0.01% $POCl_3$ and 0.01% STMP, seemed to withstand processing at higher temperatures. Furthermore, swollen granules were observed after heating at 95 ºC for 15 min compared to the images of native WCS. Small amounts of cross-linker reacted with the native starch granule resulted in a granule that did not disrupt during heating. However, the granule seemed to disintegrate into small pieces after shear treatment.

From the microscope images, it is clear that WCS cross-linked with 0.01% of $POCl_3$ had greater effect in creating chemical bonds, possible due to the faster reaction time of $POCl_3$, than the WCS reacted with 0.01% STMP. The increase of phosphate groups in the cross-linked WCS enhanced hydration of the starch granule, which resulted in an increase in the swelling property (Kaur et al., 2006; Lim & Seib, 1993).

Increasing the amount of cross-linker reacted in the WCS granule, 0.1% $POCl_3$ and 1% STMP, restricted more the swelling of the granule during heating, possible due to the increase of inter-molecular and intra-molecular bonding in the highly cross-linked WCS (Kaur et al., 2006; Yoneya et al., 2003). After shaking the low-concentration pastes prepared with high concentration of cross-linker, it could be observed that the granules were disrupted, and higher number of remnants were left. Higher amount of crosslinker, enhanced the ability of the granule to withstand severe process conditions, e.g. heat and shear.

For specimens collected from RVA preparation, an increase of the degree of integrity was observed with increasing amounts of crosslinker agent in the WCS for both cross-linker agents. An increase of the amount of cross-linker also influenced paste transparency after RVA treatment. In addition, samples with higher amount of crosslinker were more turbid. A high number of intact granules were observed in the samples containing higher amount of cross-linker (Figure 3).

4.3.4 Fluorescence intensity of CCVJ in low-concentration dispersions of native and chemically modified waxy corn starch

Fluorescence intensity of CCVJ was measured at microliter level of gelatinized native WCS, WCS cross-linked with STMP and $POCl_3$, and ClearJel® (Figure 4.4 and 4.5).

4.3.4.1 Fluorescence intensity of CCVJ in low-concentration dispersions crosslinked WCS with STMP.

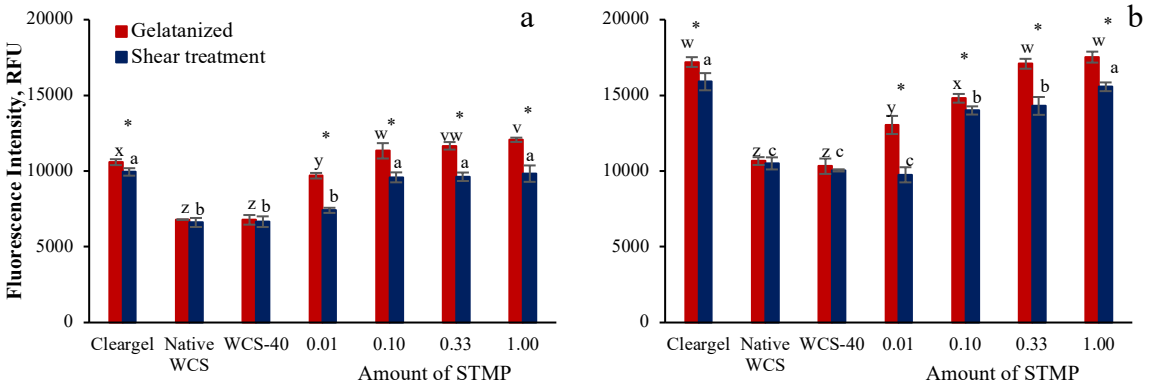

Figure 4.4 Fluorescence intensity of CCVJ in non-shaken (red bars) and shaken (blue bars) dispersions of native waxy corn starch and its derivatives. Cross-linked waxy corn starch was prepared by reacting it with sodium trimetaphosphate (STMP). Control samples were prepared by treating WCS with the same reaction condition as the crosslinked samples (WCS-40). A commercially available crosslinked waxy corn starch (ClearJel®) is included for comparison. Dispersions were prepared at 0.5% (a) and 1% (b) starch concentration and shaken at 30000 RPM for 10 min. Fluorescence intensity of CCVJ was recorded with an excitation/emission wavelength of 440 nm and 500 nm, respectively. Different letters mean significant difference within samples before shaking (v, w, x, y, and z) and within samples after shaking (a, b, c, d, and e). Asterisk (*) means significant difference before and after shaking.

For both starch concentration tested, 0.5% and 1%, the fluorescence intensity of CCVJ increased with increasing amount of cross-linker in the modified sample. The lower fluorescence intensity was recorded for the native WCS and WCS treated with the same conditions as the crosslinked samples for both starch concentrations. Furthermore, the fluorescence intensity of CCVJ in WCS prepared at 1% was higher than the starch prepared at 0,5%, which means that the amount of free volume in the sample was affected with concentration of starch.

When subjected to shear treatment, no significant difference was found in the shaken and non-shaken WCS samples for both concentrations. When the native WCS and treated WCS granules were heated at 95 ºC there was a high swelling of granules. Addition of iodine in the cooled gelatinized paste, resulted in a slight staining (Figure 4.3). The swollen granules were loose and with large free volume in their structure. When subjected to shear treatment, the granules of these WCS samples were completely disrupted and the loose structure was no longer visible under

microscope. However, it was noticed that the free volume in the shaken starch granules was not affected and the signal of CCVJ was similar for both WCS samples.

When the WCS was cross-linked with 0.01% of STMP there was an increase in the CCVJ signal after gelatinization. It was observed that the introduction of lower amount of crosslinker kept the integrity of the granule after heat treatment (Figure 4.3). However, the swollen granule was still loose. After shaking this starch pastes, the fluorescence intensity of CCVJ was reduced and was similar to the CCVJ signal registered for the native WCS. It can be observed from microscope images (Figure 4.3), that this slightly cross-linked WCS was completely disrupted after shear treatment. It is likely that the number of covalent bonds incorporated with the small amount of STMP to WCS granule increased the heat-resistant property of the granule but did not confer any shear-resistant property.

The fluorescence emission of CCVJ increased with increasing amounts of the cross-linker in the modified WCS. The highest fluorescence intensity registered for both starch concentration was for WCS cross-linked with 1% STMP. After shear treatment, a reduction of the CCVJ signal was observed. The signal in samples prepared at 0.5% had no significant difference for all three samples cross-linked with high amounts of STMP. In the pastes prepared at 1%, the higher signal of CCVJ was registered for the sample cross-linked with 1% STMP. It could be seen from microscope images (Figure 4.3) that the increase of cross-linker resulted in a more restricted-swollen granule after heat treatment. After shear treatment, a high number of granule remnants could be observed. It is likely that the cross-linking of WCS with higher amount of STMP resulted in a granule with high number of internal chemical bridges and hence a granule with restricted free volume. By increasing the amount of cross-linker, stiffer nano-structures may have been formed which further restricted the internal rotation of CCVJ and increased the emission of photons through fluorescence intensity.

4.3.4.2 Fluorescence intensity of CCVJ in low-concentration dispersions of WCS crosslinked with $POCl_3$.

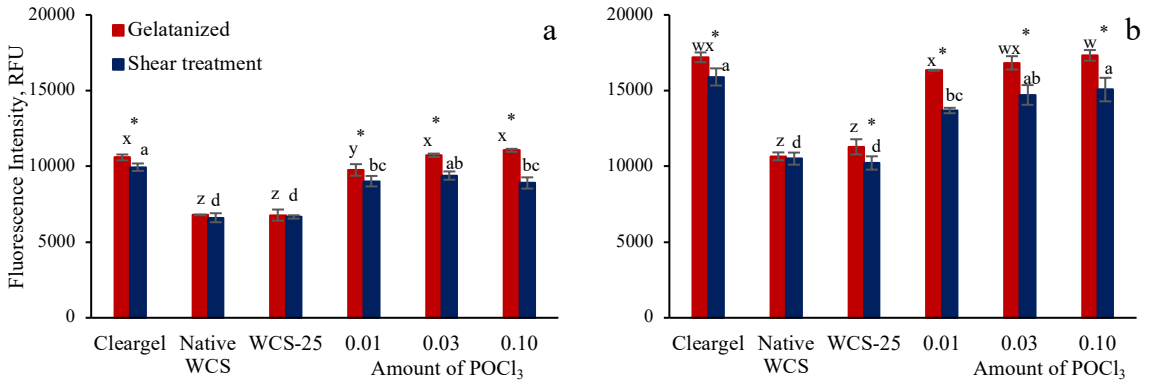

Figure 4.5 Fluorescence intensity of CCVJ in non-shaken (red bars) and shaken (blue bars) dispersions of native waxy corn starch and its derivatives. Cross-linked waxy corn starch was prepared by reacting it and phosphoryl oxychloride ($POCl_3$). Control samples were prepared by treating WCS with the same reaction condition as the cross-linked samples (WCS-25). A commercially available crosslinked waxy corn starch (ClearJel®) is included for comparison. Dispersions were prepared at 0.5% (a) and 1% (b) starch concentration and shaken at 30000 RPM for 10 min. Fluorescence intensity of CCVJ was recorded with an excitation/emission wavelength of 440 nm and 500 nm, respectively. Different letters mean significant difference within samples before shaking (v, w, x, y, and z) and within samples after shaking (a, b, c, d, and e). Asterisk (*) means significant difference before and after shaking.

The fluorescence intensity of the WCS and WCS with similar conditions as the cross-linked samples with $POCl_3$ (WCS-25) were non-significative after heat and shear treatments. The fluorescence intensity of CCVJ increased when a higher amount of cross-linker agent was introduced in the modified WCS. After shear treatments, the signal of CCVJ was lower in the shaken starch granules. It could also be observed from microscope images (Figure 4.3) and fluorescence intensity measurements (Figure 4.5) that WCS treated with lower amounts of $POCl_3$, 0.01%, resulted in stiffer granule after shear treatment that those obtained with 0.01% of STMP. The reduction in CCVJ signal was lower in WCS cross-linked with 0.01% $POCl_3$ compared to WCS reacted with 0.01% STMP. Reaction of $POCl_3$ with starch was described as fast and occurring mainly on the surface of the granule (Hirsch & Kokini, 2002). This rapid reaction in the outer layer of granule, makes the granule stiffer and consequently a network with restricted volume.

In previous reports, Loutfy, (1986), Jee et al. (2009), Gavvala et al. (2013), Jee, Bae, & Lee (2010), Lee et al., (2014), and Alhassawi et al. (2018) reported that the TICT state of

molecular rotors is affected not only by changes in micro-viscosity, but also the free space and the mechanical properties of the media. Furthermore, an increase in the stiffness or elastic modulus (Young's modulus) of films made of different polymers resulted in a reduction of the internal motion of the molecular rotor structure.

In general, the effect of cross-linking in starch granule is associated mainly with its swelling behavior. The higher the degree of cross-linking the more restricted the swelling will be (Kaur et al., 2006; Liu, Ramsden, & Corke, 1999; Koo, Lee, & Lee, 2010). Furthermore, a higher dependence of swelling power of starch granules is reported for the fast reacting $POCl_3$ than the slow reacting STMP (Hirsch & Kokini, 2002). Lastly, crosslinking increases the mechanical properties of the starch granule by increasing the storage and loss moduli (Bohlin, Eliasson, & Mita, 1986; Heo et al., 2017).

These results suggest that higher amount of cross-linking agent reacted in the WCS granule may result in a granule with stiffer nano-structure structure and reduced internal free volume due to the higher inter-molecular and intramolecular bridges formed. Therefore, changes in the nano-structure of WCS granules can be detected by recording changes in fluorescence emission of the CCVJ.

4.4 Conclusions

Shear-resistance of starch granules can be detected with the new protocol developed. The suitability of the high-throughput method has been evaluated. Moreover, fluorescence intensity of molecular rotor, CCVJ, was affected by the media containing diverse molecular crowding. Different amounts of phosphorus-containing agents were used to prepare cross-linked starch granules. This resulted in the likely increase of the molecular weight and molecular crowdedness inside the granule by introducing intra-molecular and inter-molecular covalent bonds. Our results show that increasing the amount of crosslinking agent used during phosphorylation of WCS resulted in a stiffer granule with reduced swelling and resistant to high-temperature and shear processing. Measurement of fluorescence intensity of CCVJ in dispersion of native and cross-linked WCS resulted in a high CCVJ signal in the dispersions prepared with cross-linked WCS with higher amount of cross-linker agent. RVA profiles of the modified WCS and microscope images of the low-concentration shaken cross-linked WCS corroborated the results obtained by measuring CCVJ signal.

REFERENCES

Abbas, J., Woodford, J., Ovel, D., Harms, D., & Jones, J. (2011). *Automated seed chipping apparatus*. Retrieved from https://www.google.com/patents/WO2011163326A2?cl=en

Abdulrazaq, S. S., Issa, S. A., & Abdulrazzak, N. J. (2015). Evaluation of the Trephine Method in Harvesting Bone Graft From the Anterior Iliac Crest for Oral and Maxillofacial Reconstructive Surgery. *Journal of Craniofacial Surgery*, *26*(8), e744. https://doi.org/10.1097/SCS.0000000000002177

Ai, Y., & Jane, J. (2018). Understanding Starch Structure and Functionality. In *Starch in Food* (pp. 151–178). https://doi.org/10.1016/B978-0-08-100868-3.00003-2

Akers, W. (2004). A Molecular Rotor as Viscosity Sensor in Aqueous Colloid Solutions. *Journal of Biomechanical Engineering*, *126*(3), 340. https://doi.org/10.1115/1.1762894

Alhassawi, F. M., Corradini, M. G., Rogers, M. A., & Ludescher, R. D. (2018). Potential applications of luminescent molecular rotors in food science and engineering. *Critical Reviews in Food Science and Nutrition*, *58*(11), 1902–1916. https://doi.org/10.1080/10408398.2017.1278583

Angellier-Coussy, H., Putaux, J.-L., Molina-Boisseau, S., Dufresne, A., Bertoft, E., & Perez, S. (2009). The molecular structure of waxy maize starch nanocrystals. *Carbohydrate Research*, *344*(12), 1558–1566. https://doi.org/10.1016/j.carres.2009.04.002

Asioli, D., Aschemann-Witzel, J., Caputo, V., Vecchio, R., Annunziata, A., Næs, T., & Varela, P. (2017). Making sense of the "clean label" trends: A review of consumer food choice behavior and discussion of industry implications. *Food Research International*, *99*, 58–71. https://doi.org/10.1016/j.foodres.2017.07.022

Banks, W., Greenwood, C. T., & Muir, D. D. (1974). Studies on Starches of High Amylose Content. Part 17. A Review of Current Concepts. *Starch - Stärke*, *26*(9), 289–300. https://doi.org/10.1002/star.19740260902

Baye, T. M., Pearson, T. C., & Settles, A. M. (2006). Development of a calibration to predict maize seed composition using single kernel near infrared spectroscopy. *Journal of Cereal Science*, *43*(2), 236–243. https://doi.org/10.1016/j.jcs.2005.11.003

Becker, S. M., & Cope, J. (2008). *Clip based sampling of seed for the removal of specific seed tissue or structures for seed analysis*. Retrieved from https://www.google.com/patents/US20080113367

Becker, S. M., Cope, J. M., Kurth, & Mongan, J. (2014). *Automated seed sampling apparatus,method and system*. Retrieved from https://www.google.com/patents/CN102686099B?cl=en

Becker, Steven M., Cope, J. M., Kurth, D., & Mongan, J. L. (2014). *United States Patent No. US8863436B2*. Retrieved from https://patents.google.com/patent/US8863436B2/en

Bemiller, J. N. (1997). Starch Modification: Challenges and Prospects. *Starch - Stärke*, *49*(4), 127–131. https://doi.org/10.1002/star.19970490402

BeMiller, J. N. (2011). Pasting, paste, and gel properties of starch–hydrocolloid combinations. *Carbohydrate Polymers*, *86*(2), 386–423. https://doi.org/10.1016/j.carbpol.2011.05.064

BeMiller, J. N. (2019). Corn Starch Modification. In *Corn* (pp. 537–549). https://doi.org/10.1016/B978-0-12-811971-6.00019-X

BeMiller, J. N., & Whistler, R. L. (Eds.). (2009). *Starch: chemistry and technology* (3. ed). London: Academic Press.

Biliaderis, C. G., & Zawistowski, J. (1990). Viscoelastic behavior of aging starch gels: effects of concentration, temperature, and starch hydrolysates on network properties. *Cereal Chemistry (USA)*, *67*(3), 240–246.

Biliaderis, Costas G. (2009). Chapter 8 - Structural Transitions and Related Physical Properties of Starch. In *Food Science and Technology*. *Starch (Third Edition)* (pp. 293–372). https://doi.org/10.1016/B978-0-12-746275-2.00008-2

Bohlin, L., Eliasson, A.-C., & Mita, T. (1986). Shear Stress Relaxation of Native and Modified Potato Starch Gels. *Starch - Stärke*, *38*(4), 120–124. https://doi.org/10.1002/star.19860380405

Boyer, C. D., & Liu, K.-C. (1985). The Interaction of Endosperm Genotype and Genetic Background. Part I. Differences in Chromatographic Profiles of Starches from Nonmutant and Mutant Endosperms. *Starch - Stärke*, *37*(3), 73–79. https://doi.org/10.1002/star.19850370302

Breedveld, V., & Pine, D. J. (2003). Microrheology as a tool for high-throughput screening. *Journal of Materials Science*, *38*(22), 4461–4470. https://doi.org/10.1023/A:1027321232318

Buléon, A., Colonna, P., Planchot, V., & Ball, S. (1998). Starch granules: structure and biosynthesis. *International Journal of Biological Macromolecules*, *23*(2), 85–112. https://doi.org/10.1016/S0141-8130(98)00040-3

Business Research Company. (2013). *Starches/Glucose: Global Markets* (No. FOD037B). Retrieved from https://www.bccresearch.com

Business Research Company. (2016). *The Global Market for Food Additives* (No. FOD009F). Retrieved from https://secure.livechatinc.com/licence/7126481/v2/open_chat.cgi?groups=3&embedded=1&newWebserv=undefined&__lc_vv=2&session_id=S1559336642.925691d842&server=secure.livechatinc.com#https://www.bccresearch.com/market-research/food-and-beverage/food-additives-market.html

Business Research Company, M. (2018). *Grain Products Market Global Briefing 2018* (No. MKB068B). Retrieved from https://www.bccresearch.com/

Cabrera-Ponce, J. L., Valencia-Lozano, E., & Trejo-Saavedra, D. L. (2019). Genetic Modifications of Corn. In *Corn* (pp. 43–85). https://doi.org/10.1016/B978-0-12-811971-6.00003-6

Cameron, D. K., & Wang, Y.-J. (2006). Application of Protease and High-Intensity Ultrasound in Corn Starch Isolation from Degermed Corn Flour. *Cereal Chemistry Journal*, *83*(5), 505–509. https://doi.org/10.1094/CC-83-0505

Chatakanonda, P., Varavinit, S., & Chinachoti, P. (2000). Effect of Crosslinking on Thermal and Microscopic Transitions of Rice Starch. *LWT - Food Science and Technology*, *33*(4), 276–284. https://doi.org/10.1006/fstl.2000.0662

Chen, M.-H., & Bergman, C. J. (2007). Method for determining the amylose content, molecular weights, and weight- and molar-based distributions of degree of polymerization of amylose and fine-structure of amylopectin. *Carbohydrate Polymers*, *69*(3), 562–578. https://doi.org/10.1016/j.carbpol.2007.01.018

Clark, A. H., & Ross-Murphy, S. B. (1987). Structural and mechanical properties of biopolymer gels. *Biopolymers*, 57–192. Springer Berlin Heidelberg.

Cogdill, R., Hurburgh, C., Rippke, G., Bajic, S., Jones, R., McClelland, J., … Liu, J. (2004). Single-Kernel Maize Analysis by Near-Infrared Hyperspectral Imaging. *Transactions of the ASAE*, 311–320.

Collison, R. (1968). *Swelling and gelatinization of starch. In starch and its derivatives. Radley JA ed*. Chapman and Hall Ltd., London, p168.

Cope, J. (2010). *Apparatus for removal of specific seed tissue or structure for seed analysis*. Retrieved from https://www.google.ch/patents/US20100044356

Cope, J. (2011). *Methods for removal of specific seed tissue or structure for seed analysis*. Retrieved from https://www.google.com/patents/US20110225680

Cope, J., & Kurth, D. (2008). *Methodologies, processes and automated devices for orientation, sampling and collections of seed tissues from individual seeds*. Retrieved from https://www.google.com/patents/US20080131924

Cope, J., Kurth, D., & Oldenburg, K. (2012). *Method, system and apparatus for removing a sample portion of a seed*. Retrieved from https://www.google.com/patents/WO2012122156A2?cl=en

Cope, J. M., Jaehnel, G. L., & Mongan, J. L. (2012). *United States Patent No. US8313053B2*. Retrieved from https://patents.google.com/patent/US8313053B2/en

Craig, S. a. S., Maningat, C. C., Seib, P. A., & Hoseney, R. C. (1989). Starch paste clarity. *Cereal Chemistry (USA)*, *3*(66), 173–182.

Darrah, L. L., McMullen, M. D., & Zuber, M. S. (2019). Chapter 2 - Breeding, Genetics and Seed Corn Production. In S. O. Serna-Saldivar (Ed.), *Corn (Third Edition)* (pp. 19–41). https://doi.org/10.1016/B978-0-12-811971-6.00002-4

Deppermann, K. L., Yannakakis, L., Singleton, A. M., Koestel, A. R., Finley, D. W., Forinash, B. J., … Schnicker, B. J. (2008). *Automated high-throughput seed sampler and methods of sampling, testing and bulking seeds*. Retrieved from https://www.google.com/patents/US20080317279

Deppermann, K. L., Zhang, Q., & Hinchey, T. B. (2014). *Automated seed sampler and methods of sampling, testing and bulking seeds*. Retrieved from https://www.google.com/patents/EP1786261B1?cl=en

Dickinson, D. B., & Preiss, J. (1969). Presence of ADP-Glucose Pyrophosphorylase in Shrunken-2 and Brittle-2 Mutants of Maize Endosperm. *Plant Physiology*, *44*(7), 1058–1062. https://doi.org/10.1104/pp.44.7.1058

Doolittle, A. K. (1952). Studies in Newtonian Flow. III. The Dependence of the Viscosity of Liquids on Molecular Weight and Free Space (in Homologous Series). *Journal of Applied Physics*, *23*(2), 236–239. https://doi.org/10.1063/1.1702182

Dowell, F. E., Pearson, T. C., Maghirang, E. B., Xie, F., & Wicklow, D. T. (2002). Reflectance and Transmittance Spectroscopy Applied to Detecting Fumonisin in Single Corn Kernels Infected with Fusarium verticillioides. *Cereal Chemistry*, *79*(2), 222–226. https://doi.org/10.1094/CCHEM.2002.79.2.222

Eerliengen, R. C., Crombez, M., & Delcour, J. A. (1993). Enzyme-resistant starch. I. Quantitative and qualitative influence of incubation time and temperature of autoclaved starch on resistant starch formation. *Cereal Chem*, *70*(3), 339–344.

Finamore, M. (2017). Momentum Behind “Clean Label” Movement Is Growing. *MMR*, *34*(1), 74–74.

Foster, J. F., & Sterman, M. D. (1956). A light scattering investigation of the retrogradation of amylose. *Journal of Polymer Science*, *21*(97), 91–101. https://doi.org/10.1002/pol.1956.120219708

Fredriksson, H., Silverio, J., Andersson, R., Eliasson, A.-C., & Åman, P. (1998). The influence of amylose and amylopectin characteristics on gelatinization and retrogradation properties of different starches. *Carbohydrate Polymers*, *35*(3), 119–134. https://doi.org/10.1016/S0144-8617(97)00247-6

Fu, Z., & BeMiller, J. N. (2017). Effect of hydrocolloids and salts on retrogradation of native and modified maize starch. *Food Hydrocolloids*, *69*, 36–48. https://doi.org/10.1016/j.foodhyd.2017.01.023

Gallant, D. J., Bouchet, B., & Baldwin, P. M. (1997). Microscopy of starch: evidence of a new level of granule organization. *Carbohydrate Polymers*, *32*(3), 177–191. https://doi.org/10.1016/S0144-8617(97)00008-8

Gavvala, K., D. Sasikala, W., Sengupta, A., A. Dalvi, S., Mukherjee, A., & Hazra, P. (2013). Modulation of excimer formation of 9-(dicyano-vinyl)julolidine by the macrocyclic hosts. *Physical Chemistry Chemical Physics*, *15*(1), 330–340. https://doi.org/10.1039/C2CP43282J

Gavvala, K., Satpathi, S., & Hazra, P. (2015). Ultrafast dynamics of a molecular rotor in chemical and biological nano-cavities. *RSC Advances*, *5*(89), 72793–72800. https://doi.org/10.1039/C5RA13298C

Gidley, M. J., & Bulpin, P. V. (1989). Aggregation of amylose in aqueous systems: the effect of chain length on phase behavior and aggregation kinetics. *Macromolecules*, *22*(1), 341–346. https://doi.org/10.1021/ma00191a062

Gray, J. A., & BeMiller, J. N. (2005). Influence of reaction conditions on the location of reactions in waxy maize starch granules reacted with a propylene oxide analog at low substitution levels. *Carbohydrate Polymers*, *60*(2), 147–162. https://doi.org/10.1016/j.carbpol.2004.11.032

Gulnov, D. V., Nemtseva, E. V., & Kratasyuk, V. A. (2016). Contrasting relationship between macro- and microviscosity of the gelatin- and starch-based suspensions and gels. *Polymer Bulletin*, *73*(12), 3421–3435. https://doi.org/10.1007/s00289-016-1664-9

Gunaratne, A., & Corke, H. (2007). Gelatinizing, Pasting, and Gelling Properties of Potato and Amaranth Starch Mixtures. *Cereal Chemistry; St. Paul*, *84*(1), 22–29.

Gutierrez, M., Volker, K. W., Vennart, R. M., & Odhav, R. (2013). J-Plasma: A New Helium Based Energy Device for Advanced Gyn Laparoscopy. *Journal of Minimally Invasive Gynecology*, *20*(6), S124. https://doi.org/10.1016/j.jmig.2013.08.421

Haidekker, M. A., L'Heureux, N., & Frangos, J. A. (2000). Fluid shear stress increases membrane fluidity in endothelial cells: a study with DCVJ fluorescence. *American Journal of Physiology-Heart and Circulatory Physiology*, *278*(4), H1401–H1406. https://doi.org/10.1152/ajpheart.2000.278.4.H1401

Haidekker, M. A., Nipper, M., Mustafic, A., Lichlyter, D., Dakanali, M., & Theodorakis, E. A. (2010). Dyes with Segmental Mobility: Molecular Rotors. In *Springer Series on Fluorescence*. *Advanced Fluorescence Reporters in Chemistry and Biology I* (pp. 267–308). https://doi.org/10.1007/978-3-642-04702-2_8

Haidekker, M. A., & Theodorakis, E. A. (2007). Molecular rotors—fluorescent biosensors for viscosity and flow. *Organic & Biomolecular Chemistry*, *5*(11), 1669–1678. https://doi.org/10.1039/B618415D

Haidekker, M. A., & Theodorakis, E. A. (2010). Environment-sensitive behavior of fluorescent molecular rotors. *Journal of Biological Engineering*, *4*, 11. https://doi.org/10.1186/1754-1611-4-11

Haidekker, M. A., Tsai, A. G., Brady, T., Stevens, H. Y., Frangos, J. A., Theodorakis, E., & Intaglietta, M. (2002). A novel approach to blood plasma viscosity measurement using fluorescent molecular rotors. *American Journal of Physiology - Heart and Circulatory Physiology*, *282*(5), H1609–H1614. https://doi.org/10.1152/ajpheart.00712.2001

Hamaker, B. R., Tuncil, Y. E., & Shen, X. (2019). Chapter 11 - Carbohydrates of the Kernel. In S. O. Serna-Saldivar (Ed.), *Corn (Third Edition)* (pp. 305–318). https://doi.org/10.1016/B978-0-12-811971-6.00011-5

Han, J.-A., & BeMiller, J. N. (2005). Rate of Hydroxypropylation of Starches as a Function of Reaction Time. *Starch - Stärke*, *57*(9), 395–404. https://doi.org/10.1002/star.200500415

Hannappel, U. (2011). *Tissue separation method*. Retrieved from https://www.google.com/patents/WO2011119763A1?cl=en

Hannappel, U. (2013). *Tissue separation method*. Retrieved from https://www.google.com/patents/US20130011843

Hawe, A., Filipe, V., & Jiskoot, W. (2010). Fluorescent molecular rotors as dyes to characterize polysorbate-containing IgG formulations. *Pharmaceutical Research*, *27*(2), 314–326. https://doi.org/10.1007/s11095-009-0020-2

Heinemann, C., Cardinaux, F., Scheffold, F., Schurtenberger, P., Escher, F., & Conde-Petit, B. (2004). Tracer microrheology of γ-dodecalactone induced gelation of aqueous starch dispersions. *Carbohydrate Polymers*, *55*(2), 155–161. https://doi.org/10.1016/j.carbpol.2003.09.003

Hennet, P. (2015). Piezoelectric Bone Surgery: A Review of the Literature and Potential Applications in Veterinary Oromaxillofacial Surgery. *Frontiers in Veterinary Science*, *2*. https://doi.org/10.3389/fvets.2015.00008

Heo, H., Lee, Y.-K., & Chang, Y. H. (2017). Rheological, pasting, and structural properties of potato starch by cross-linking. *International Journal of Food Properties*, *20*(sup2), 2138–2150. https://doi.org/10.1080/10942912.2017.1368549

Hirsch, J. B., & Kokini, J. L. (2002). Understanding the Mechanism of Cross-Linking Agents (POCl3, STMP, and EPI) Through Swelling Behavior and Pasting Properties of Cross-Linked Waxy Maize Starches. *Cereal Chemistry Journal*, *79*(1), 102–107. https://doi.org/10.1094/CCHEM.2002.79.1.102

Holder, D. G., Glover, D. V., & Shannon, J. C. (1974). Interaction of Shrunken-2 with Five Other Carbohydrate Genes in Corn Endosperm 1. *Crop Science*, *14*(5), 643–646. https://doi.org/10.2135/cropsci1974.0011183X001400050010x

Hoover, R., Hughes, T., Chung, H. J., & Liu, Q. (2010). Composition, molecular structure, properties, and modification of pulse starches: A review. *Food Research International*, *43*(2), 399–413. https://doi.org/10.1016/j.foodres.2009.09.001

Ikawa, Y., Glover, D. V., Sugimoto, Y., & Fuwa, H. (1981). Some Structural Characteristics of Starches of Maize Having a Specific Genetic Background. *Starch - Stärke*, *33*(1), 9–13. https://doi.org/10.1002/star.19810330105

Inouchi, N., Glover, D. V., Sugimoto, Y., & Fuwa, H. (1991). DSC Characteristics of Gelatinization of Starches of Single-, Double-, and Triple-Mutants and Their Normal Counterpart in the Inbred Oh43 Maize (Zea mays L.) Background. *Starch - Stärke*, *43*(12), 468–472. https://doi.org/10.1002/star.19910431205

Jacobsen, N. E. (2007). *NMR spectroscopy explained: simplified theory, applications and examples for organic chemistry and structural biology*. Hoboken, N.J: Wiley-Interscience.

Jacobson, M. R., & BeMiller, J. N. (1998). Method for Determining the Rate and Extent of Accelerated Starch Retrogradation. *Cereal Chemistry Journal*, *75*(1), 22–29. https://doi.org/10.1094/CCHEM.1998.75.1.22

Jacobson, M. R., Obanni, M., & Bemiller, J. N. (1997). Retrogradation of Starches from Different Botanical Sources. *Cereal Chemistry Journal*, *74*(5), 511–518. https://doi.org/10.1094/CCHEM.1997.74.5.511

Jane, J., Chen, Y. Y., Lee, L. F., McPherson, A. E., Wong, K. S., Radosavljevic, M., & Kasemsuwan, T. (1999). Effects of Amylopectin Branch Chain Length and Amylose Content on the Gelatinization and Pasting Properties of Starch [1]. *Cereal Chemistry*, *76*(5), 629–637. https://doi.org/10.1094/CCHEM.1999.76.5.629

Jane, Jay-lin. (2009). Chapter 6 - Structural Features of Starch Granules II. In *Food Science and Technology*. *Starch (Third Edition)* (pp. 193–236). https://doi.org/10.1016/B978-0-12-746275-2.00006-9

Jankowski, T. (1992). Influence of starch retrogradation on the texture of cooked potato tuber. *International Journal of Food Science & Technology*, *27*(6), 637–642. https://doi.org/10.1111/j.1365-2621.1992.tb01233.x

Janni, J., Weinstock, B. A., Hagen, L., & Wright, S. (2008). Novel near-infrared sampling apparatus for single kernel analysis of oil content in maize. *Applied Spectroscopy*, *62*(4), 423–426. https://doi.org/10.1366/000370208784046885

Jee, A.-Y., Bae, E., & Lee, M. (2009). Internal Twisting Dynamics of Dicyanovinyljulolidine in Polymers. *The Journal of Physical Chemistry B*, *113*(52), 16508–16512. https://doi.org/10.1021/jp908430w

Jee, A.-Y., Bae, E., & Lee, M. (2010). Internal motion of an electronically excited molecule in viscoelastic media. *The Journal of Chemical Physics*, *133*(1), 014507. https://doi.org/10.1063/1.3454724

Ji, Y., Seetharaman, K., & White, P. J. (2004). Optimizing a Small-Scale Corn-Starch Extraction Method for Use in the Laboratory. *Cereal Chemistry Journal*, *81*(1), 55–58. https://doi.org/10.1094/CCHEM.2004.81.1.55

Jyothi, A. N., Moorthy, S. N., & Rajasekharan, K. N. (2006). Effect of Cross-linking with Epichlorohydrin on the Properties of Cassava (Manihot esculenta Crantz) Starch. *Starch - Stärke*, *58*(6), 292–299. https://doi.org/10.1002/star.200500468

Kasemsuwan, T., & Jane, J. L. (1996). Quantitative method for the survey of starch phosphate derivatives and starch phospholipids by 31P nuclear magnetic resonance spectroscopy. *Cereal Chemistry (USA)*. Retrieved from http://agris.fao.org/agris-search/search.do;jsessionid=E7CFE8EF8831905E8734C6F66379CBB4?request_locale=fr&recordID=US9716478&query=&sourceQuery=&sortField=&sortOrder=&agrovocString=&advQuery=&centerString=&enableField=

Kasemsuwan, T., & Jane, J. (1994). Location of amylose in normal starch granules. II. Locations of phosphodiester cross-linking revealed by phosphorus-31 nuclear magnetic resonance. *Cereal Chemistry (USA)*. Retrieved from http://agris.fao.org/agris-search/search.do?recordID=US9501994

Kaufman, R. C., Wilson, J. D., Bean, S. R., Herald, T. J., & Shi, Y.-C. (2015). Development of a 96-well plate iodine binding assay for amylose content determination. *Carbohydrate Polymers*, *115*, 444–447. https://doi.org/10.1016/j.carbpol.2014.09.015

Kaur, L., Singh, J., & Singh, N. (2006). Effect of cross-linking on some properties of potato (Solanum tuberosum L.) starches. *Journal of the Science of Food and Agriculture*, *86*(12), 1945–1954. https://doi.org/10.1002/jsfa.2568

Keetels, C. J. A. M., van Vliet, T., & Walstra, P. (1996). Gelation and retrogradation of concentrated starch systems: 1 Gelation. *Food Hydrocolloids*, *10*(3), 343–353. https://doi.org/10.1016/S0268-005X(96)80011-7

Koo, S. H., Lee, K. Y., & Lee, H. G. (2010). Effect of cross-linking on the physicochemical and physiological properties of corn starch. *Food Hydrocolloids*, *24*(6), 619–625. https://doi.org/10.1016/j.foodhyd.2010.02.009

Kung, C. E., & Reed, J. K. (1989). Fluorescent molecular rotors: a new class of probes for tubulin structure and assembly. *Biochemistry*, *28*(16), 6678–6686. https://doi.org/10.1021/bi00442a022

Kuribayashi-Shigetomi, K., Takahashi, R., Subagyo, A., Sueoka, K., & Okajima, T. (2015). High-throughput Measurements of Single Cell Rheology by Atomic Force Microscopy. In T. Arai, F. Arai, & M. Yamato (Eds.), *Hyper Bio Assembler for 3D Cellular Systems* (pp. 57–67). https://doi.org/10.1007/978-4-431-55297-0_4

Labanca, M., Azzola, F., Vinci, R., & Rodella, L. F. (2008). Piezoelectric surgery: Twenty years of use. *British Journal of Oral and Maxillofacial Surgery*, *46*(4), 265–269. https://doi.org/10.1016/j.bjoms.2007.12.007

Lee, S.-K., Ramer, S., & Toppozada, A. (2010). *Patent No. WO/2010/141263*. Retrieved from https://patentscope.wipo.int/search/en/detail.jsf?docId=WO2010141263&recNum=233&docAn=US2010036028&queryString=(FP/quantum)%2520&maxRec=2958

Lee, Y., Kim, Y. L., Kim, M. H., & Lee, M. (2014). Fluorescence imaging of nanobiomaterials: Thioflavin T in electrospun poly(vinyl alcohol) fibres. *International Journal of Nanotechnology*, *11*(5–678), 502–508. https://doi.org/10.1504/IJNT.2014.060571

Lehmann, L., Kudryashov, E., & Buckin, V. (2004). Ultrasonic monitoring of the gelatinisation of starch. In M. Miguel & H. D. Burrows (Eds.), *Trends in Colloid and Interface Science XVI* (pp. 136–140). Springer Berlin Heidelberg.

Lim, S., & Seib, P. A. (1993). Preparation and pasting properties of wheat and corn starch phosphates. *Cereal Chemistry*. Retrieved from http://agris.fao.org/agris-search/search.do?recordID=US19940103186

Liu, H., Ramsden, L., & Corke, H. (1999). Physical properties and enzymatic digestibility of hydroxypropylated ae, wx, and normal maize starch. *Carbohydrate Polymers*, *40*(3), 175–182. https://doi.org/10.1016/S0144-8617(99)00052-1

Liu, Huijun, Ramsden, L., & Corke, H. (1999). Physical Properties of Cross-linked and Acetylated Normal and Waxy Rice Starch. *Starch - Stärke*, *51*(7), 249–252. https://doi.org/10.1002/(SICI)1521-379X(199907)51:7<249::AID-STAR249>3.0.CO;2-O

Loutfy, R. O. (1986). Fluorescence Probes for Polymer Free-Volume. In *NATO ASI Series*. *Photophysical and Photochemical Tools in Polymer Science* (pp. 429–448). https://doi.org/10.1007/978-94-009-4726-9_19

Loutfy, R. O., & Arnold, B. A. (1982). Effect of viscosity and temperature on torsional relaxation of molecular rotors. *The Journal of Physical Chemistry*, *86*(21), 4205–4211. https://doi.org/10.1021/j100218a023

Loutfy, R. O., & Teegarden, D. M. (1983). Effect of polymer chain tacticity on the fluorescence of molecular rotors. *Macromolecules*, *16*(3), 452–456. https://doi.org/10.1021/ma00237a022

Lumdubwong, N., & Seib, P. A. (2000). Rice Starch Isolation by Alkaline Protease Digestion of Wet-milled Rice Flour. *Journal of Cereal Science*, *31*(1), 63–74. https://doi.org/10.1006/jcrs.1999.0279

MacKintosh, F. C., & Schmidt, C. F. (1999). Microrheology. *Current Opinion in Colloid & Interface Science*, *4*(4), 300–307. https://doi.org/10.1016/S1359-0294(99)90010-9

Mansky, P., & Hajduk, D. A. (2004). *Patent No. US6769292 B2*. Retrieved from http://www.google.ch/patents/US6769292

Martinant, J. P., Zhang, D., Zuber, A., & Maisonneuve, J. P. (2015). *Seed tissue sampling process*. Retrieved from https://www.google.com/patents/WO2015110472A1?cl=en

Mathieson, A., Wallace, R., Cleary, R., Li Li, null, Simpson, H., & Lucas, M. (2017). Ultrasonic Needles for Bone Biopsy. *IEEE Transactions on Ultrasonics, Ferroelectrics, and Frequency Control*, *64*(2), 433–440. https://doi.org/10.1109/TUFFC.2016.2633286

Matignon, A., & Tecante, A. (2017). Starch retrogradation: From starch components to cereal products. *Food Hydrocolloids*, *68*, 43–52. https://doi.org/10.1016/j.foodhyd.2016.10.032

McDonagh, P. (2012). 7 - Native, modified and clean label starches in foods and beverages. In D. Baines & R. Seal (Eds.), *Natural Food Additives, Ingredients and Flavourings* (pp. 162–174). https://doi.org/10.1533/9780857095725.1.162

Morrison, W. R. (1964). A fast, simple and reliable method for the microdetermination of phosphorus in biological materials. *Analytical Biochemistry*, *7*(2), 218–224. https://doi.org/10.1016/0003-2697(64)90231-3

Moschakis, T. (2013). Microrheology and particle tracking in food gels and emulsions. *Current Opinion in Colloid & Interface Science*, *18*(4), 311–323. https://doi.org/10.1016/j.cocis.2013.04.011

Ninomya, Y., Okuno, K., Glover, D. V., & Fuwa, H. (1989). Some Properties of Starches of Sugary-1; Brittle-1 Maize (Zea mays L.). *Starch - Stärke*, *41*(5), 165–167. https://doi.org/10.1002/star.19890410502

Nipper, M. E., Majd, S., Mayer, M., Lee, J. C.-M., Theodorakis, E. A., & Haidekker, M. A. (2008). Characterization of changes in the viscosity of lipid membranes with the molecular rotor FCVJ. *Biochimica Et Biophysica Acta*, *1778*(4), 1148–1153. https://doi.org/10.1016/j.bbamem.2008.01.005

Peng, X., & Yao, Y. (2018). Small-granule starches from sweet corn and cow cockle: Physical properties and amylopectin branching pattern. *Food Hydrocolloids*, *74*(Supplement C), 349–357. https://doi.org/10.1016/j.foodhyd.2017.08.025

Puchongkavarin, H., Varavinit, S., & Bergthaller, W. (2005). Comparative Study of Pilot Scale Rice Starch Production by an Alkaline and an Enzymatic Process. *Starch - Stärke*, *57*(3–4), 134–144. https://doi.org/10.1002/star.200400279

Qiu, S., Yadav, M. P., Chen, H., Liu, Y., Tatsumi, E., & Yin, L. (2015). Effects of corn fiber gum (CFG) on the pasting and thermal behaviors of maize starch. *Carbohydrate Polymers*, *115*, 246–252. https://doi.org/10.1016/j.carbpol.2014.08.071

Ratnayake, W. S., & Jackson, D. S. (2008). Chapter 5 Starch Gelatinization. In *Advances in Food and Nutrition Research* (Vol. 55, pp. 221–268). https://doi.org/10.1016/S1043-4526(08)00405-1

Ring, S. G. (1987). Molecular interactions in aqueous solutions of the starch polysaccharides: a review. *Food Hydrocolloids*, *1*(5), 449–454. https://doi.org/10.1016/S0268-005X(87)80039-5

Ring, Stephen G., Colonna, P., I'Anson, K. J., Kalichevsky, M. T., Miles, M. J., Morris, V. J., & Orford, P. D. (1987). The gelation and crystallisation of amylopectin. *Carbohydrate Research*, *162*(2), 277–293. https://doi.org/10.1016/0008-6215(87)80223-9

Russell, P. L., Berry, C. S., & Greenwell, P. (1989). Characterisation of resistant starch from wheat and maize. *Journal of Cereal Science*, *9*(1), 1–15. https://doi.org/10.1016/S0733-5210(89)80017-7

Rutenberg, M. W., & Solarek, D. (1984). STARCH DERIVATIVES: PRODUCTION AND USES. In *Starch: Chemistry and Technology* (pp. 311–388). Retrieved from http://linkinghub.elsevier.com/retrieve/pii/B9780127462707500161

Sang, Y., Prakash, O., & Seib, P. A. (2007). Characterization of phosphorylated cross-linked resistant starch by 31P nuclear magnetic resonance (31P NMR) spectroscopy. *Carbohydrate Polymers*, *67*(2), 201–212. https://doi.org/10.1016/j.carbpol.2006.05.009

Sangtong, V., Mottl, E. C., Long, M. J., Lee, M., & Scott, M. P. (2001). Serial extraction of endosperm drillings (SEED)—A method for detecting transgenes and proteins in single viable maize kernels. *Plant Molecular Biology Reporter*, *19*(2), 151–158. https://doi.org/10.1007/BF02772157

Sawada, S., Iio, T., Hayashi, Y., & Takahashi, S. (1992). Fluorescent rotors and their applications to the study of G-F transformation of actin. *Analytical Biochemistry*, *204*(1), 110–117.

Schultz, K. M., & Furst, E. M. (2011). *High-throughput rheology in a microfluidic device*. *11*(22), 3802–3809. https://doi.org/10.1039/C1LC20376B

Shannon, J. C., Garwood, D. L., & Boyer, C. D. (2009). Chapter 3 - Genetics and Physiology of Starch Development. In J. BeMiller & R. Whistler (Eds.), *Starch (Third Edition)* (pp. 23–82). https://doi.org/10.1016/B978-0-12-746275-2.00003-3

Silverio, J., Fredriksson, H., Andersson, R., Eliasson, A.-C., & Åman, P. (2000). The effect of temperature cycling on the amylopectin retrogradation of starches with different amylopectin unit-chain length distribution. *Carbohydrate Polymers*, *42*(2), 175–184. https://doi.org/10.1016/S0144-8617(99)00140-X

Sullivan, J. W., & Johnson, J. A. (n.d.). Measurement of Starch Gelatinization by Enzyme Susceptibility. *Cereal Chem*, (41), 73–79.

Tallada, J. G., Palacios-Rojas, N., & Armstrong, P. R. (2009). Prediction of maize seed attributes using a rapid single kernel near infrared instrument. *Journal of Cereal Science*, *50*(3), 381–387. https://doi.org/10.1016/j.jcs.2009.08.003

Tanackovic, V., Rydahl, M. G., Pedersen, H. L., Motawia, M. S., Shaik, S. S., Mikkelsen, M. D., … Blennow, A. (2016). High throughput screening of starch structures using carbohydrate microarrays. *Scientific Reports*, *6*, 30551. https://doi.org/10.1038/srep30551

Tassieri, M. (2019). Microrheology with optical tweezers: peaks & troughs. *Current Opinion in Colloid & Interface Science*, *43*, 39–51. https://doi.org/10.1016/j.cocis.2019.02.006

Tattiyakul, J., & Rao, M. A. (2000). Rheological behavior of cross-linked waxy maize starch dispersions during and after heating. *Carbohydrate Polymers*, *43*(3), 215–222. https://doi.org/10.1016/S0144-8617(00)00160-0

Vamadevan, V., & Bertoft, E. (2015). Structure-function relationships of starch components. *Starch - Stärke*, *67*(1–2), 55–68. https://doi.org/10.1002/star.201400188

Vamadevan, V., & Bertoft, E. (2018). Impact of different structural types of amylopectin on retrogradation. *Food Hydrocolloids*, *80*, 88–96. https://doi.org/10.1016/j.foodhyd.2018.01.029

Viriot, M. L., Carré, M. C., Geoffroy-Chapotot, C., Brembilla, A., Muller, S., & Stoltz, J. F. (1998). Molecular rotors as fluorescent probes for biological studies. *Clinical Hemorheology and Microcirculation*, *19*(2), 151–160.

Wang, L., & Wang, Y.-J. (2001). Comparison of Protease Digestion at Neutral pH with Alkaline Steeping Method for Rice Starch Isolation. *Cereal Chemistry*, *78*(6), 690–692. https://doi.org/10.1094/CCHEM.2001.78.6.690

Wang, L., & Wang, Y.-J. (2004). Rice starch isolation by neutral protease and high-intensity ultrasound. *Journal of Cereal Science*, *39*(2), 291–296. https://doi.org/10.1016/j.jcs.2003.11.002

Wang, S., Li, C., Copeland, L., Niu, Q., & Wang, S. (2015). Starch Retrogradation: A Comprehensive Review: Starch retrogradation…. *Comprehensive Reviews in Food Science and Food Safety*, *14*(5), 568–585. https://doi.org/10.1111/1541-4337.12143

Wang, Y.-J. (1992). Characterization of starch structures and properties of maize mutants from the Oh43 inbred line. *Retrospective Theses and Dissertations*. https://doi.org/10.31274/rtd-180813-12504

Weil, C. F., & Monde, R.-A. (2007). Induced mutations in maize. *Israel Journal of Plant Sciences*, *55*(2), 183–190. https://doi.org/10.1560/IJPS.55.2.183

Whistler, R. L., Smith, R. J., Wolfrom, M. L., & BeMiller, J. N. (1964). *Methods in carbohydrate chemistry. Volume 4, Volume 4,*. New York(N.Y.); Londres (GB): Academic Press.

Wiesenborn, D. P., Orr, P. H., Casper, H. H., & Tacke, B. K. (1994). Potato Starch Paste Behavior as Related to Some Physical/Chemical Properties. *Journal of Food Science*, *59*(3), 644–648. https://doi.org/10.1111/j.1365-2621.1994.tb05583.x

Wongsagonsup, R., Pujchakarn, T., Jitrakbumrung, S., Chaiwat, W., Fuongfuchat, A., Varavinit, S., … Suphantharika, M. (2014). Effect of cross-linking on physicochemical properties of tapioca starch and its application in soup product. *Carbohydrate Polymers*, *101*, 656–665. https://doi.org/10.1016/j.carbpol.2013.09.100

Woo, K. S., & Seib, P. A. (2002). Cross-Linked Resistant Starch: Preparation and Properties. *Cereal Chemistry Journal*, *79*(6), 819–825. https://doi.org/10.1094/CCHEM.2002.79.6.819

Woo, K., & Seib, P. A. (1997). Cross-linking of wheat starch and hydroxypropylated wheat starch in alkaline slurry with sodium trimetaphosphate. *Carbohydrate Polymers*, *33*(4), 263–271. https://doi.org/10.1016/S0144-8617(97)00037-4

Wu, J. S., Goldsmith, J. D., Horwich, P. J., Shetty, S. K., & Hochman, M. G. (2008). Bone and Soft-Tissue Lesions: What Factors Affect Diagnostic Yield of Image-guided Core-Needle Biopsy? *Radiology*, *248*(3), 962–970. https://doi.org/10.1148/radiol.2483071742

Yang, N., Lv, R., Jia, J., Nishinari, K., & Fang, Y. (2017). Application of Microrheology in Food Science. *Annual Review of Food Science and Technology*, *8*(1), 493–521. https://doi.org/10.1146/annurev-food-030216-025859

Yao, Y., Guiltinan, M. J., Shannon, J. C., & Thompson, D. B. (2002). Single Kernel Sampling Method for Maize Starch Analysis While Maintaining Kernel Vitality. *Cereal Chemistry Journal*, *79*(6), 757–762. https://doi.org/10.1094/CCHEM.2002.79.6.757

Yeh, A. I., & Yeh, S. L. (1993). Some characteristics of hydroxypropylated and cross-linked rice starch. *Cereal Chemistry (USA)*. Retrieved from http://agris.fao.org/agris-search/search.do?recordID=US9433823

Yoneya, T., Ishibashi, K., Hironaka, K., & Yamamoto, K. (2003). Influence of cross-linked potato starch treated with POCl3 on DSC, rheological properties and granule size. *Carbohydrate Polymers*, *53*(4), 447–457. https://doi.org/10.1016/S0144-8617(03)00143-7

Yue Li, Shoemaker, C. F., Xueran Shen, Jianguo Ma, Ibáñez-Carranza, A. M., & Fang Zhong. (2008). The Isolation of Rice Starch with Food Grade Proteases Combined with Other Treatments. *Food Science and Technology International*, *14*(3), 215–224. https://doi.org/10.1177/1082013208092824

Zhao, J., Chen, Z., Jin, Z., de Waard, P., Buwalda, P., Gruppen, H., & Schols, H. A. (2015). Level and position of substituents in cross-linked and hydroxypropylated sweet potato starches using nuclear magnetic resonance spectroscopy. *Carbohydrate Polymers*, *131*, 424–431. https://doi.org/10.1016/j.carbpol.2015.06.005

Zhong, Z., & Sun, X. S. (2005). Thermal characterization and phase behavior of cornstarch studied by differential scanning calorimetry. *Journal of Food Engineering*, *69*(4), 453–459. https://doi.org/10.1016/j.jfoodeng.2004.07.023

Zhou, X., Baik, B.-K., Wang, R., & Lim, S.-T. (2010). Retrogradation of waxy and normal corn starch gels by temperature cycling. *Journal of Cereal Science*, *51*(1), 57–65. https://doi.org/10.1016/j.jcs.2009.09.005